Available online at www.sciencedirect.com
SCIENCE DIRECT®
Chemical Physics 314 (2005) 263–282
Chemical Physics
www.elsevier.com/locate/chemphys

Photoion mass spectrometry of adenine, thymine and uracil in the 6–22 eV photon energy range

Hans-Werner Jochims [a], Martin Schwell [b], Helmut Baumgärtel [a], Sydney Leach [c,*]

[a] Institut für Physikalische und Theoretische Chemie der Freien Universität Berlin, Takustr. 3, 14195 Berlin, Germany
[b] Laboratoire Interuniversitaire des Systèmes Atmosphériques (LISA), CNRS-UMR 7583, Universités Paris 7 et 12, 61 Avenue du Général de Gaulle, 94010 Créteil, France
[c] Laboratoire d'Etude du Rayonnement et de la Matière en Astrophysique (LERMA), CNRS-UMR 8112, Observatoire de Paris-Meudon, 5 place Jules-Janssen, 92195 Meudon, France

Received 8 February 2005; accepted 16 March 2005
Available online 12 April 2005

Abstract

Using synchrotron radiation as excitation source in the 6–22 eV photon energy region, a photoionization mass spectrometry study of three nucleic acid bases, adenine, thymine and uracil, revealed VUV-induced degradation pathways of these important biological molecules. The fragmentation patterns, ionization energies and ion appearance energies (AE) are reported, many for the first time, and are compared with results of electron impact and other studies. AE values enabled heats of formation of parent and some fragment ions to be revised or determined for the first time. Thermochemical data, coupled with the observed AEs, were also useful in clarifying dissociative photoionization pathways. The main neutral loss species are HCN for adenine, HNCO and CO for thymine and uracil, but many subsequent and other fragmentation pathways, including some not suggested previously, are observed and discussed. The hyperconjugation properties of the methyl group make CO loss easier in thymine than in uracil. The astrophysically important fragment ion $HCNH^+$ is shown to be formed by several fragmentation pathways in all three nucleobases. The relative importance of competitive fragmentation processes was determined in some cases. Some astrophysical implications concerning the prospects for observation and survival of these nucleic acid bases in the interstellar medium and in meteorites are briefly discussed.

1. Introduction

The vacuum ultraviolet (VUV) photophysics and photochemistry of the pyrimidine and purine nucleic acid base constituents of DNA is of considerable interest in view of the possible delivery of these molecules from space to the early Earth, and the role that they could have played in the origin and development of life on our planet [1]. Some nucleobases have been found in meteorites [2–5], speculation has been made concerning their possible formation in the interstellar medium (ISM) [6,7], and pyrimidines and purines have been reported in the data obtained with the PUMA impact mass spectrometer during the flyby of comet Halley by the Soviet spacecraft VEGA 1 [8]. Gas phase studies of nucleic acid bases are also of significance in biology for understanding and determining properties of these basic units when free from interactions.

Concerning their possible existence in an astrophysical context, the observation of the important nucleobases by radioastronomy requires initial laboratory studies on their gas phase microwave spectra, which have indeed been carried out for the major tautomers

* Corresponding author. Tel.: +33 1 4507 7561; fax: +33 1 4507 7100.
E-mail address: sydney.leach@obspm.fr (S. Leach).

0301-0104/$ - see front matter © 2005 Elsevier B.V. All rights reserved.
doi:10.1016/j.chemphys.2005.03.008

of the three nucleic acid bases studied here, adenine [9], thymine [10] and uracil [11]. Other possibilities of astrophysical observation include their infra-red spectra, which have been measured in the laboratory in the gas phase [12] and in low temperature matrices [13–16], both phases being relevant to possible astrophysical measurements. Gas phase electronic spectra are also known, but the observed UV absorption [17–19] or fluorescence [20,21] bands would be difficult to measure and identify in astrophysical contexts. However, all of these spectroscopic studies have enriched our knowledge of the structure of these nucleobases in their tautomeric variants. Mass spectrometric measurements of cometary grains, already attempted on comet Halley in 1986 [8], will be improved in future space missions to comets, with some specific attempts to detect purine nucleobases [22].

Although the nucleobases studied possess several tautomeric forms, the spectroscopic studies cited above show that at the gas phase temperatures used in our study, 150–200 °C, only one tautomer is present, at more than 99%, with no evidence of tautomerization of uracil or thymine to the enol form, or of adenine to the imino form [12].

Apart from several photoelectron spectral studies [23–31] there has been relatively little previous study of ionization phenomena of adenine, thymine and uracil. Their adiabatic ionization energies are uncertain and there are only a small number of mass spectral studies on unmodified nucleobases, carried out by 20 and 70 eV electron impact, principally by the group of Dudek [32,33], followed by others [34–41]. No dissociative photoionization studies have been reported on these nucleobases. We mention that there has been recent work on the dissociative electron attachment of nucleobases and on their stable anions in the gas phase [42,43]. We also note that energetic fragments resulting from dissociation of nucleobases can cause subsequent damage in biological systems. DeVries et al. [44] have studied the fragmentation of uracil and thymine induced by collision with slow multiply charged Xe(q+, q = 5–25) ions. Complete breakdown into atomic and diatomic fragments occurs via Coulomb dissociation under these conditions.

In this paper, we report results of a photoionization mass spectrometry (PIMS) study of three nucleic acid bases, adenine, thymine and uracil. All three have been found in meteoritic materials [2–5]. The photoion yield curves of the nucleic acid base parent and fragment ions were measured as a function of incident photon energy in the 6–22 eV range. We report ionization energy (IE) and previously unknown fragment appearance energies (AE). Knowledge of the ionization energies of the nucleobases is of importance in understanding the processes of oxidative damage [45,46], as well as in interpreting hole (radical cation) charge transfer and trapping [47–49], in DNA. The photoion fragmentation patterns at an incident energy of 20 eV are compared with the ion fragmentation patterns obtained by 20 and 70 eV electron impact ionization processes. Our proposed fragmentation pathways build on the pioneer studies of Rice et al. [32,33] on the electron impact mass spectra of these nucleobases. These pathways were established in part by making use of metastable peaks and isotope labeling [34–37]. Our measurements of the appearance energies of fragment ions enable us to further investigate the validity of the proposed fragmentation pathways and to consider new aspects and extensions of the dissociative ionization processes. The fragmentation information is not only pertinent to understanding radiation damage in DNA [50] but, as mentioned above, it is also potentially of use for interpretation of data to be obtained by mass spectrometric measurements of species in cometary grains which will be collected during the ROSETTA space mission to the comet 46p/Wirtanen [22].

The photoabsorption cross-section of nucleic acid bases is much higher in the VUV as compared with the UV, as has been observed in absorption and EELS studies on films of nucleobases, usually prepared by vacuum sublimation [51–55]. Low energy EELS measurements have been carried out on gas phase thymine [56], and high energy EELS on solid films of the three nucleobases studied here, which provided data up to 35 eV [57]. We later compare this data, as well as photoelectron spectra, with our nucleobase parent photoion yield curves. MPI spectra of gas phase adenine have also been measured [18]. Optical properties of adenine in the 1.8–80 eV region have been determined by optical reflectance on solid films [58]. Photoacoustic spectra of films of thymine and adenine have also been obtained and compared with absorption measurements in the 4.13–9.54 eV range [59]. In these different studies the bands observed have been assigned to π–π*, n–π*, etc. transitions and to chromophoric groups. We also note the existence of a broad intense ''absorption'' peak of the nucleobases in the 20 eV region. This results mainly from collective excitation of electrons and is commonly observed in organic compounds, as discussed elsewhere [60].

We mention that all of these molecules absorb strongly at 10.2 eV, where the Lyman-α stellar emission is intense. Furthermore, in connection with the possible earthbound delivery of biotic molecules from space, we remark that the VUV luminosity of the early sun, during the Hadean period of considerable bombardment of the Earth from space, was about two orders of magnitude higher than it is today, although the total luminosity was less [61].

Initial accounts of this work, which have been reported elsewhere in an exobiology context [62,63], include preliminary values of the ionization energies and

some fragmentation appearance energies of the three nucleobases [62].

2. Experimental

The experiments were carried out at two separate synchrotron facilities, BESSY I and BESSY II, in Berlin. Synchrotron radiation from the electron storage ring BESSY I was monochromatized by a 1.5 m Au grating monochromator (modified McPherson) and then focused into a differentially pumped gas cell which can be heated up to 400 °C but was here restricted to lower temperatures. The experimental set-up is described in more detail elsewhere [64]. The nucleic acid base vapors were introduced into the ionization chamber by direct evaporation of solid samples in open containers placed 1–2 cm below the position of the incident VUV radiation within the ion extraction zone. The whole chamber was heated to temperatures, typically 120–140 °C, which provided an adequate supply of target molecules but were sufficiently low to ensure that the thermally fragile low volatile nucleic acid bases remained essentially undissociated in the gas phase. When some thermally induced dissociation did occur this was easily identified by the observed mass spectra, thus enabling us to modify experimental parameters so as to achieve satisfactory experimental conditions of minimal thermal dissociation. In cases where water impurity was observed in the mass spectra this generally resulted from residues of cleaning procedures of the apparatus which were carried out between experimental runs.

Parent and fragment ions formed by photoionization of the nucleic acid bases adenine, thymine and uracil were measured using a quadrupole mass spectrometer (Leybold Q200), and ion yield curves were obtained through photon energy scans with measuring intervals of 25 meV. The yield curves of the principal ions observed are presented in the appropriate figures. Transmitted photons were detected by the fluorescence of a sodium salicylate coated window. Spectral bandwidth of the incident monochromatic radiation was typically 2 Å. Some experiments were carried out with an MgF_2 filter (cut-off effective at 11.0 eV) in order to suppress stray light and second-order radiation. Ion appearance energies were determined mainly with the aid of semi-log plots of the ion yield curves. A second set of measurements on uracil was carried out more recently using synchrotron radiation from the BESSY II electron storage ring. Measuring equipment and experimental conditions were similar to those at BESSY I, except that at BESSY II we employed a 3 m normal incidence monochromator. The nucleic acid base samples were commercial products (Sigma–Aldrich) of best available purity. The formulae of the three nucleobases studied are given in Fig. 1.

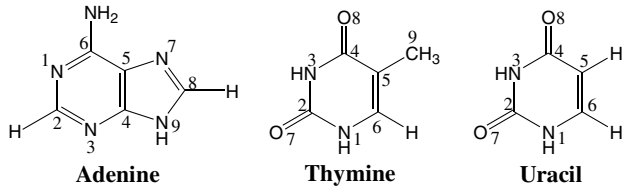

Fig. 1. Molecular structure of adenine, thymine and uracil, including common atom numbering.

3. Results and discussion

3.1. Adenine: mass spectra and ion yield curves

Table 1 gives a comparison between the relative intensities of the m/z peaks in our mass spectrum obtained at 20 eV photon excitation energy and that of Rice and Dudek [33] measured with 70 eV electron impact. It also includes selected proposed loss of neutral species corresponding to the observed molecular ions formed by dissociative ionization. The appearance energies of the major m/z ions are listed, as measured from the onsets in the ion yield curves (Fig. 2).

The 20 eV photon impact and 70 eV electron impact mass spectra have essentially the same m/z features but with differences in their relative intensities. Different relative intensities are also observed between reported electron impact mass spectra of adenine [22,33,38,65]. These differences between the electron impact spectra, and also between electron and photon impact mass spectra, are most probably mainly due to different ion optics, residence times, and detection efficiency. These factors will affect the mass spectral manifestations, especially of metastable ions. We remark also that with 70 eV electron impact, but not with 20 eV photons, doubly charged molecular ions can be formed, with low yields, giving rise to charge separation reactions producing fragment monocations [66]. Differences between reported electron impact mass spectral intensities were also observed for thymine and uracil, as discussed later.

3.1.1. The adenine parent ion

For the parent ion, $m/z = 135$, we measured an ionization energy of 8.20 ± 0.03 eV. The corresponding $m/z = 135$ ion yield curve shown in Fig. 2(a) was measured using the MgF_2 filter. In Table 2 this value is compared with those determined by various techniques. The only other measurement by photoionization is that reported Orlov et al. [67], who did not publish their ion yield curve. Agreement between these two PIMS measurement is good. An early measurement by electron impact [68] gives a much too high value, but later measurements [69,70] are not inconsistent with our IE value. A recent measurement by the R2PI technique gives an upper limiting value 400 meV above the PIMS values [71]. The ionization energies reported from photoelectron

Table 1
Electron impact [33] and photon impact mass spectra and photoion appearance energies: Adenine $m = 135$ ($C_5H_5N_5$)

m/z	Electron impact 70 eV relative intensity	Photon impact 20 eV relative intensity	Photon impact appearance energy (AE, eV)	Ion elemental formula	Neutral loss
135	100	100	8.20 ± 0.03	$C_5H_5N_5^+$	
134	3	10		$C_5H_4N_5^+$	H
120	3	1		$C_5H_4N_4^+$	NH
119	(a)	3		$C_5H_3N_4^+$	NH_2
108	34	57	11.56 ± 0.05	$C_4H_4N_4^+$	HCN
107	3	10		$C_4H_3N_4^+$	H_2CN
92	(a)	9		$C_4H_2N_3^+$	$HCN + NH_2$
81	19	50	12.8 ± 0.1	$C_3H_3N_3^+$	2HCN
80	7	10		$C_3H_2N_3^+$	$H_2CN + HCN$
70	5	17	13.1 ± 0.1	$C_2H_4N_3^+$	C_3NH_2
67	7	10		$C_3H_3N_2^+$	HCN + NHCN
66	15	41	13.2 ± 0.1	$C_3H_2N_2^+$	$HCN + NH_2CN$
65	6	0		$C_3HN_2^+$	$2HCN + NH_2$
54	31	55	13.7 ± 0.1	$C_2H_2N_2^+$	3HCN
53	24	28		$C_2HN_2^+$	$H_2CN + 2HCN$
43	12	34	13.0 ± 0.1	NH_2CNH^+	HCN + HCNCCN
42	3	16		NH_2CN^+	
41	2	7		$NHCN^+$	
40	5	1		NCN^+	2HCN + NHCN
39	8	1		$HCCN^+$	$2HCN + NH_2CN$
38	10	0		C_2N^+	$3HCN + NH_2$
29	12	60	14.0 ± 0.1	NH_2CH^+	
28	78	110	13.1 ± 0.1	$HCNH^+$	$C_4H_3N_4$
27	12	10		HCN^+	4HCN

(a) Reported in [65] and in [38] but not in [33].

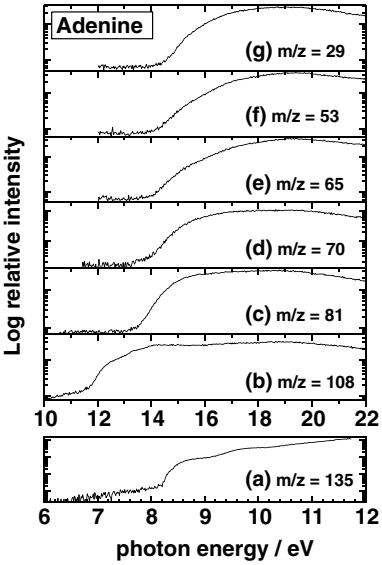

Fig. 2. Selected ion yield curves of adenine. The $m/z = 135$ ion yield curve has been measured using an MgF_2 cut-off filter.

spectroscopy peak measurements [23,31] provide vertical IEs which are 220–280 meV above the adiabatic values determined by our PIMS measurements. However, bracketing experiments measuring the adiabatic recombination energy [72] gave an adiabatic IE = 8.55 ± 0.10 eV, about 350 meV above the PIMS value, and which is close to the vertical IE measured by photoelectron spectroscopy. This points to unrecognized difficulties in the recombination energy measurement technique.

The difference of the order of 250 meV between the adiabatic and vertical IEs of adenine is similar to that calculated theoretically with various degrees of sophistication [73–76]. There is no loss of planarity on ionization of adenine [74]. The difference between the adiabatic and vertical IEs therefore reflects bond length and angle changes (which have been calculated by Improta et al. [75]), between the ground states of neutral and cationic adenine, and which result in Franck–Condon transition shifts. It may appear surprising that electron impact measurements are capable of providing adiabatic values of the ionization energy in cases where there are significant changes in the geometry of neutral species on electron loss, but this has been well demonstrated for many molecular species [77].

Using our measured adiabatic IE of adenine, and the known value of the heat of formation ΔH_f^{298} (adenine) $= 207 \pm 8$ kJ/mol [78], we obtain a value of the heat of formation of the cation ΔH_f^{298} (adenine cation) $= 998 \pm 11$ kJ/mol, which is considerably greater than the value ΔH_f^{298} (adenine cation) $= 960$ kJ/mol given by Lias et al. [78], based on a quoted PES onset value of the IE = 7.8 eV.

We made a direct comparison between the $m/z = 135$ ion yield curve and the HeI photoelectron spectrum of

Table 2
Adenine ionization energy values[a]

Experimental method	Ionization energy (eV)	Reference and year
Photoion yield curve (PIMS)	8.20 ± 0.03	Present study
Electron impact ion yield curve	8.91 ± 0.10	[68] 1967
Photoelectron spectroscopy (PES)	8.44 ± 0.03 (vert)	[23] 1975
PIMS	8.26 ± 0.05	[67] 1976
Electron impact ion yield curve	8.3 ± 0.1	[69] 1976
PES	8.48[b] (vert)	[31] 1980
Electron impact ion yield curve	8.45 ± 0.15	[70] 1996
Recombination energy	8.55 ± 0.10	[72] 1999
Resonance 2-photon ionization	$\leqslant 8.606 \pm 0.006$	[71] 2002

[a] Adiabatic values unless otherwise stated.
[b] Uncertainty not reported.

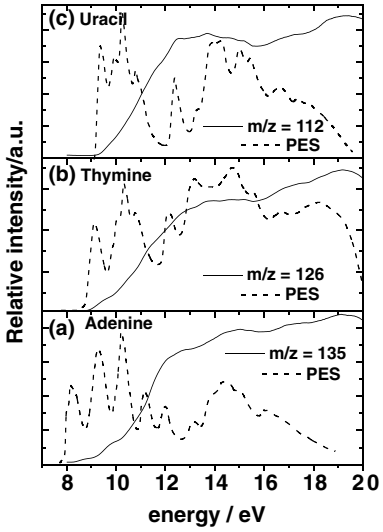

Fig. 3. Comparison of parent ion yield curve and photoelectron spectrum (PES are reproduced from [24,31]): (a) adenine; (b) thymine; (c) uracil.

adenine measured by Lin et al. [31] (Fig. 3(a)). This showed clearly that there are shoulders or apparent steps in the ion yield curve at energies close to those of several features in the photoelectron spectrum (PES energies [24,31] in brackets): 8.4 (8.48) eV assigned to π_1; ~9.0 (−) eV; ~9.8 (9.6) eV assigned to n_1 and π_2; ~10.3 (10.5) eV assigned to π_3; ~12.0 (12.1) eV assigned to π_4. The molecular orbital assignments are those given in the PES studies [24,31]. The inflection that we observe clearly in the ion yield curve at ~9.0 eV has no obvious feature in the photoelectron spectra of adenine. However, the 9.6 eV PES feature is broad and its profile extends to about 8.8 eV on the lower energy side. This PES feature has been assigned to both n_1 and π_2 and their energy separation has been calculated to be 450 meV by the HAM/3 method and 780 meV by 4-31G calculations [24], although the order of these two orbitals differs in the two calculations. On the basis of relative intensities in the PES spectrum, we assign the 9.0 eV inflection in the adenine ion yield curve to the n_1 orbital and the 9.8 eV inflection to π_2.

At higher energies, the broad features in the PES between 13 and 17 eV mimic quite well the parent ion yield curve (Fig. 3(a)). This region of the PES has not been assigned but we note that there are similar features in the PES of purine in this energy region, for which molecular orbital assignments have been made [79]. We recall that the purine molecule is similar to that of adenine but in which the amino group of the latter is replaced by a hydrogen atom.

We also compared the parent ion yield curve with the optical absorption curve derived from 25 keV electron energy loss spectra of thin films of adenine [57] (Fig. 4(a)). Our parent ion yield curves has several features, including three pronounced peaks at ~14.5, ~16 and ~18 eV, respectively. There are only two peaks, at 13 ± 0.3 and 17.4 ± 0.3 eV, in the adenine film spectrum in the 10–35 eV region. The physical relation between these solid phase peaks, induced by electron excitation in a region where the ionization yield can be less than unity [80,81], and the gas phase parent photoion peaks in this spectral region is not easy to disentangle.

3.1.2. Adenine ion fragmentation

Several loss mechanism pathways can be recognized in the mass spectrum, following on the pioneer work of the Dudek group [33]. A schematic representation of major fragmentation pathways is given in Fig. 5.

(α) *Successive loss of HCN groups:* The principal pathway involves the successive loss of HCN ($m = 27$) groups:

$$C_5H_5N_5^+ \ (m/z = 135) - HCN \rightarrow C_4H_4N_4^+ \ (m/z = 108) \quad (1)$$

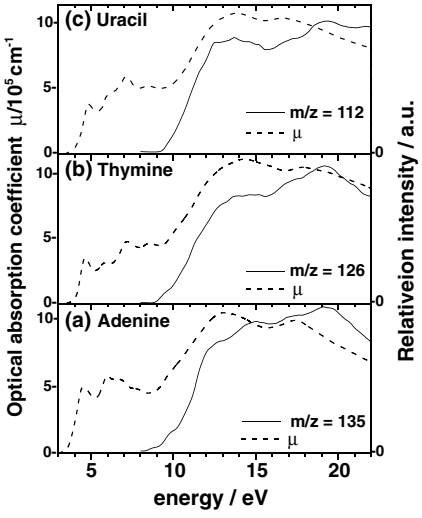

Fig. 4. Comparison of parent ion yield curve and the optical photoabsorption spectrum (the optical absorption spectra, reproduced from [57], are derived from respective electron energy loss spectra): (a) adenine; (b) thymine; (c) uracil.

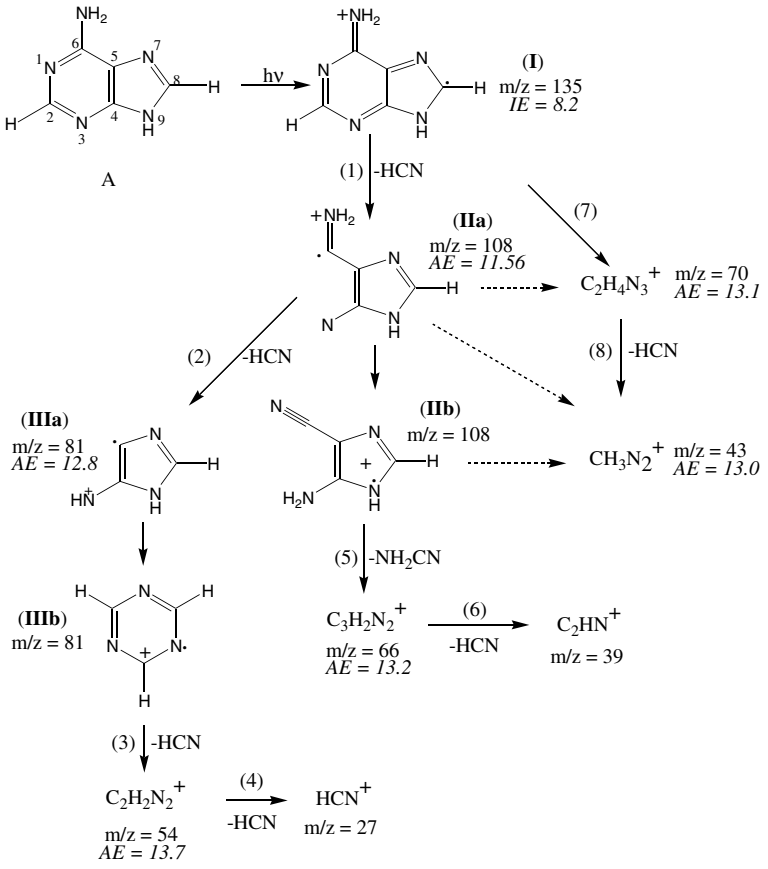

Fig. 5. Principal fragmentation decay routes of the adenine radical cation. Measured appearance energy values are given for each fragment (in eV, for uncertainties refer to Table 1). Roman and Arabic numerals correspond to species and reactions, respectively.

$$C_4H_4N_4^+ \ (m/z = 108) - HCN \rightarrow C_3H_3N_3^+ \ (m/z = 81) \tag{2}$$

$$C_3H_3N_3^+ \ (m/z = 81) - HCN \rightarrow C_2H_2N_2^+ \ (m/z = 54) \tag{3}$$

$$C_2H_2N_2^+ \ (m/z = 54) - HCN \rightarrow HCN^+ \ (m/z = 27) \tag{4}$$

From the appearance energy of the $C_4H_4N_4^+$ ion, AE = 11.56 eV, and the known heats of formation of adenine (207 ± 8 kJ/mol) and HCN (135.1 kJ/mol) [65,78], we calculate the heat of formation of the $C_4H_4N_4^+$ ion to be 1187 ± 12 kJ/mol. A similar calculation for the heat of formation of the $C_3H_3N_3^+$ ion gave a value of 1172 ± 16 kJ/mol for this ion. The heats of formation of the three isomeric cyclic $C_3H_3N_3^+$ ions, 1,2,3-triazine, 1,2,4-triazine and 1,3,5-triazine, are reported [65,78] to be 1313, 1222 and 1194 kJ/mol, respectively. This suggests that the $C_3H_3N_3^+$ ion formed in the dissociative ionization of adenine is the 1,3,5-triazine cation (species IIIb in Fig. 5).

The respective appearance energies of the $C_nH_nN_n^+$ ($n = 5, 4, 3, 2$) ions are 8.20, 11.56, 12.8 and 13.7 eV. Loss of the successive HCN groups requires excess energies, respectively, of 3.36, 4.5 and 5.4 eV in the ion. This suite of AEs and the corresponding excess energies confirms the pathway presented above. The initial HCN fragmentation, which requires at least two bond ruptures, is relatively more difficult than the succeeding HCN losses which each probably requires only one bond rupture in the precursor fragment ion and/or it corresponds to a successively smaller total reorganization energy. The loss mechanisms could be quite complex and may involve loss of HNC as well as HCN. Our discussion does not distinguish between these two isomers. We refer to them collectively as HCN.

From electron impact mass spectra of deuterium labeled adenine [35] Occolowitz concluded that the first HCN lost originates 55% from C6 and its attached amine group, and 45% from C2 and either adjacent nitrogen. However, the mass spectra of ^{15}N-labeled adenines [36] showed that there is about 87% loss of N1 in the first HCN product, which suggests that a greater percentage of C2 is lost than reported by Occolowitz. The finding by Barrio et al. [36] is corroborated by the electron impact mass spectrum of ^{13}C2-adenine by Sethi et al. [37] which shows that the carbon atoms in the first

HCN molecule to be lost are 98% from C2. The main reaction would therefore be expected to occur by rupture of the C2–N3 and N1–C6 bonds. These are both calculated to be weaker in the cation as compared with neutral adenine, whereas the C2–N1 and N3–4 bonds are calculated to be stronger in the cation [75].

The ^{15}N mass spectra [36] also show that N7 and N9 are completely retained in the $C_4H_4N_4^+$ ion product. Sethi et al. [37] also found, from the mass spectrum of $^{14}C8$-adenine, that there is complete retention of C8 in the $C_4H_4N_4^+$ ion formed by the first HCN loss process, and that there is partial loss of the carbon isotopic label in further HCN loss steps. We note, however, that there can be rearrangements of hydrogen (deuterium) prior to HCN leaving the molecule, as discussed by Sethi et al. [37]. Furthermore, many fragmentation sub-pathways can indeed be envisaged to contribute to these successive HCN loss processes [33,37].

From these earlier isotopic studies, we can thus assume that fragment $m/z = 108$ has the structure IIa shown in Fig. 5. Species IIa can isomerize to give species IIb which is probably thermodynamically more stable. It is not clear from which structure the $m/z = 81$ ion is formed, but, as already concluded from thermodynamical considerations, the 1,3,5 triazine cation IIIb is most likely formed.

(β) *Reactions involving loss of NH_2CN and NHCN:* Several other fragmentation pathways can be established from the mass spectrum of adenine. One of these starts from the $C_4H_4N_4^+$ fragment ion ($m/z = 108$) which can lose NH_2CN to form the important $C_2H_2N_2^+$ ion ($m/z = 66$), from which there can be a further loss of HCN:

$$C_4H_4N_4^+ \ (m/z = 108) \rightarrow C_3H_2N_2^+ \ (m/z = 66) + NH_2CN \ (m = 42) \quad (5)$$

$$C_3H_2N_2^+ \ (m/z = 66) \rightarrow C_2N^+ \ (m/z = 39) + HCN \ (m = 27) \quad (6)$$

The heat of formation of the $C_3H_2N_2^+$ ion can be determined from its appearance energy, $AE = 13.2 \pm 0.1$ eV, and the heats of formation of NH_2CN, HCN and adenine. The heats of formation of three isomers of NH_2CN have been reported [65,78]: (i) cyanamide (134 kJ/mol), (ii) diazomethane (230 ± 17 kJ/mol) and (iii) 3H-diazirine (265 ± 11 kJ/mol). These provide the following respective values for the heat of formation of $C_2H_2N_2^+$: (i) 1212 ± 16 kJ/mol, (ii) 1116 ± 33 kJ/mol, and (iii) 1081 ± 27 kJ/mol. The only heat of formation reported for a $C_2H_2N_2^+$ ion is that of the malononitrile ion, 1491 ± 11 kJ/mol [65]. This is much greater than the above values and it shows that $C_2H_2N_2^+$ is not the malononitrile ion which, if formed by dissociative ionization of adenine, would have an appearance energy several eV above 13.2 eV. The structure of the $C_2H_2N_2^+$ ion formed at 13.2 eV is therefore unknown.

Loss of NH_2CN from $m/z = 81$ constitutes another possible pathway to form the C_2HN^+ ($m/z = 39$) ion other than via reactions (5) and (6) which involve the $m/z = 66$ ion. The $m/z = 66$ and 81 ions are both intense in our 20 eV photon impact mass spectrum, but the $m/z = 39$ ion, although present, is extremely weak. The three ions, $m/z = 81$, 66 and 39, appear with modest intensity in 70 eV electron impact mass spectra [33,38,65], where their intensities decrease in the m/z order $81 > 66 > 39$, but with the $I(66)/I(39)$ intensity ratio being of the order of 2. This is undoubtedly due to the greater deposition of energy at the higher excitation energies in the electron impact case. The appearance energy of the $m/z = 66$ ion (13.2 eV, Table 1), formed by losses of HCN and NH_2CN (reactions (1) and (5)), is greater than that of $m/z = 81$ (12.8 eV), which involves loss of two HCN units from the parent ion (reactions (1) and (2)). The difference ΔE between the heat of formation of HCN and those of the NH_2CN isomers cyanamide, diazomethane and 3H-Diazirine is, respectively, $\Delta E = 0.01$, -0.98 and -1.35 eV. The difference between the appearance energies of the $m/z = 81$ and $m/z = 66$ ions is -0.4 eV, which indicates that the NH_2CN neutral product is cyanamide and that there is a potential barrier, at least of the order of 0.4 eV, to its formation.

One can imagine another formation pathway for the $m/z = 66$ ion: by rupture of the C5–C6 bond and the C4–N3 bond in the adenine parent ion. This remains to be tested, but the $AE = 13.2$ eV of the $m/z = 66$ ion is compatible with such a mechanism.

We remark that direct loss of NH_2CN from the parent ion would give a fragment ion $m/z = 93$, which is absent in our 20 eV photon impact mass spectrum. Its formation would involve rupture of three bonds and thus require a high internal energy in the parent ion, consistent with the non observation of this fragment ion in our mass spectrum. It is reported as a very weak peak in some [38,65] 70 eV electron impact mass spectra. We note the existence of an important peak at $m/z = 42$, which we assign to the NH_2CN^+ ion, and which might be formed by the dissociation $C_4H_4N_4^+ \rightarrow NH_2CN^+ + C_3H_2N_2$, which itself constitutes a charge-switch reaction relative to reaction (5). From the suggested structure IIb (Fig. 5) of the $m/z = 108$ ion, the NH_2CN^+ fragment is either the cyanamide or 3H-Diazirine cation, requiring H-shift for their formation, and not the diazomethane cation the formation of which would necessitate more complex atomic rearrangements.

(γ) *Other important ions:* The existence of a strong peak at $m/z = 43$ ($AE = 13.0$ eV) is of interest. We propose its assignment to an ion having the elemental formula $CH_3N_2^+$, in agreement with Sethi et al. [37]. It has been suggested that possible pathways to its formation involve prior formation of the $m/z = 70$ ion:

$$C_5H_5N_5^+ \ (m/z = 135) \rightarrow C_2H_4N_3^+ \ (m/z = 70) + C_3HN_2 \ (m = 65) \quad (7)$$

$$C_2H_4N_3^+ \ (m/z = 70) \rightarrow C_3HN_2^+ \ (m/z = 43) + HCN \ (m = 27) \quad (8)$$

The high resolution mass spectrometry of adenine has shown the $m/z = 70$ ion to have the elemental formula $C_2H_4N_3^+$, suggested to be formed by loss of C_3HN_2 from the parent ion [37]. We consider that there could also be a pathway to this $m/z = 70$ ion via $m/z = 108$, where the neutral loss from the latter ion would be C_2N (reaction (9)). This is a previously unreported fragmentation pathway:

$$C_4H_4N_4^+ \ (m/z = 108) \rightarrow C_2H_4N_3^+ \ (m/z = 70) + C_2N(m = 38) \quad (9)$$

The $m/z = 70$ ion has an appearance energy $AE = 13.1 \pm 0.1$ eV. From this, and appropriate heats of formation, we determine the heat of formation of this $C_2H_4N_3^+$ ion via reactions (9) and (8) to be 980 ± 18 kJ/mol. In the literature [78] there is reported a heat of formation of 835 kJ/mol for a cyclic radical ion having the elemental formula $C_2H_4N_3^+$. If this is indeed the $m/z = 70$ ion, a potential barrier can be inferred for the formation of this ion fragment via reactions (9) and (8). An open chain form is also possible, as suggested by Sethi et al. [37].

We note that the intensity of the $m/z = 70$ ion relative to that of $m/z = 43$ is about 0.5 in both the photon and electron impact mass spectra, and that both ions have closely similar AE values, which suggests that there exist more than one pathway to form the $m/z = 43$ ion. Indeed, we propose another possible pathway for its formation. This is via the $m/z = 108$ ion in the following way: If the $C_4H_4N_4^+$ ion is in its amino-imidazole carbonitrile form (species IIb in Fig. 5), subsequent rupture of C=C and a C–N bond would lead to the formation of the NH_2CNH^+ (i.e., $CH_3N_2^+$) ion.

$m/z = 28$ and $m/z = 29$ ions: These are prominent ions and their relative importance is much greater in the 20 eV photon impact than in the 70 eV electron impact mass spectrum. The $m/z = 29$ ion has an $AE = 14.0$ eV. Its elemental formula is CH_3N^+ and it is possibly the NH_2CH^+ ion [82,83]. The $m/z = 28$ ion is very intense and it has an $AE = 13.1$ eV. We assign it to the $HCNH^+$ species. Since its AE is lower than the AE of the $m/z = 29$ ion, it is not formed, at threshold, by loss of a hydrogen atom from the latter. A possibility is that the $HCNH^+$ ion is formed by the reaction:

$$C_5H_5N_5^+ \ (m/z = 135) \rightarrow HCNH^+ \ (m/z = 28) + C_4H_3N_4 \ (m = 107) \quad (10)$$

which would correspond to a charge switch of reaction Eq. (11), discussed below. However, other pathways to formation of the $HCNH^+$ ion are possible, as indicated by ^{15}N-labeled adenine studies [37].

(δ) *Less intense fragment ion peaks (no AE measurements):* The $m/z = 134$, 120, 119 and 118 ions, which are variously observed weakly in some electron impact mass spectra [22,33,38,65], correspond, respectively, to loss of H, NH, NH_2, and NH_3 groups. The corresponding reactions would leave the condensed heteroaromatic system undestroyed (if N10 is part of the leaving group). The $m/z = 120$ ion is reported in the electron impact mass spectra by Rice and Dudek [33] and Varmuza et al. [22] but not the $m/z = 119$ and 118 ions, while the spectra reported by McCloskey [38] and in the NIST collection [65] contain the $m/z = 118$ and 119 peaks, but not the $m/z = 120$ feature. Only $m/z = 134$, 120 and 119 were observed, in our 20 eV photon impact spectra. Observations of H and NH_n loss processes in the dissociative ionization of adenine are thus sensitively dependent on the source and ion optics parameters in mass spectrometers used in the measurements.

Another fragmentation pathway involves the initial loss of H_2CN (methylene-amidogen) to give the fragment ion $m/z = 107$. This is followed by successive loss of one HCN unit to form the ion $m/z = 80$, and another HCN loss to give the $m/z = 53$ ion.

$$C_5H_5N_5^+ \ (m/z = 135) \rightarrow C_4H_3N_4^+ \ (m/z = 107) + H_2CN \ (m = 28) \quad (11)$$

$$C_4H_3N_4^+ \ (m/z = 107) \rightarrow C_3H_2N_3^+ \ (m/z = 80) + HCN \ (m = 27) \quad (12)$$

$$C_3H_2N_3^+ \ (m/z = 80) \rightarrow C_2HN_2^+ \ (m/z = 53) + HCN \ (m = 27) \quad (13)$$

The relatively small intensities of the corresponding mass peaks in both electron and photon impact mass spectra show that this is a minor pathway. Occolowitz [35] observed that only about 35% of the ^{14}C label is retained in the fragment ions $m/z = 80$ formed by loss of HCN and H_2CN from the parent ion, which is a similar percentage to that observed in the $m/z = 81$ ions formed by loss of two HCN groups from $m/z = 135$. He also suggested that the existence of an intermediate ion that could lose either HCN or H_2CN.

We note also that the existence of a peak at $m/z = 92$, whose intensity, relative to that of $m/z = 119$, indicates that it arises from loss of NH_2 (or H + NH) from $m/z = 108$ rather than the suggested [37] loss of HCN from $m/z = 119$. The $m/z = 65$ and 38 ions which also involve loss of NH_2, following multiple loss of HCN groups from the parent ion, are observed only in electron impact mass spectra (Table 1). Finally, we also mention ions $m/z = 67$ and 40, which involve loss of NHCN, following initial loss, respectively, of one and two HCN units from the parent ion. We note also the

existence of a peak at $m/z = 41$, corresponding to the $NHCN^+$ ion.

3.2. Thymine: mass spectra and ion yield curves

In Table 3, the relative intensities of the m/z peaks in our thymine mass spectrum, obtained at 20 eV photon excitation energy, are compared with those of Rice et al. [32], measured with both 20 and 70 eV electron impact. The appearance energies of the major m/z ions are listed, as measured from the onsets in the photoion yield curves (Fig. 6), as well as the neutral loss species which we consider to be formed with the observed m/z ions by dissociative ionization.

Just as in the case of adenine, the 20 eV photon impact and 70 eV electron impact mass spectra of thymine are closely similar, having essentially the same m/z features but with a few differences in their relative intensities. The $m/z = 55$ fragment ion peak is the strongest in both cases, the parent peak at $m/z = 126$ being about half as intense. Other 70 eV electron impact mass spectra of thymine have been reported [34,38,65], which also have the $m/z = 126$, 83, 55, 54 and 28 peaks as the most intense, but which have different relative intensities from those measured by Rice et al. [32]. As mentioned earlier, these differences between the electron impact spectra are most probably mainly due to differences in the ion optics and ion residence times.

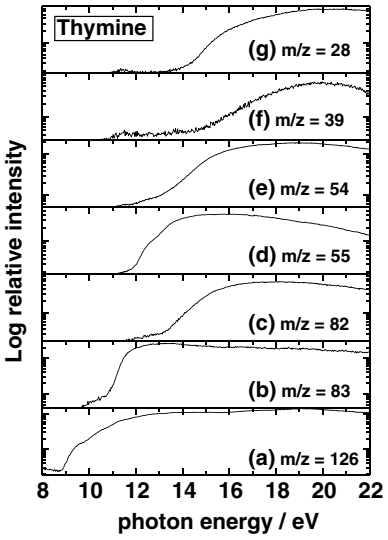

Fig. 6. Selected ion yield curves of thymine.

We note that a 20 eV electron impact mass spectrum of thymine has the parent peak as its most intense ion. The relative paucity of the mass spectral peaks in the

Table 3
Electron impact [32] and photon impact mass spectra and photoion appearance energies: Thymine $m = 126$ ($C_5H_6N_2O_2$)

m/z	Electron impact 70 eV relative intensity	Electron impact 20 eV relative intensity	Photon impact 20 eV relative intensity	Photon impact appearance energy (AE, eV)	Ion elemental formula	Neutral loss
126	46	100	52	8.82 ± 0.03	$C_5H_6N_2O_2^+$	
125	0	0	2		$C_5H_5N_2O_2^+$	H
97	2	0	1		$C_4H_3NO_2^+$	NH_2CH
84	2	2	3		$C_4H_6NO^+$	NCO
83	6	17	8	10.70 ± 0.05	$C_4H_5NO^+$	HNCO
82	7	4	10	13.20 ± 0.05	$C_4H_4NO^+$	HNCO + H
71	3	0	3		$OCNHCO^+$	CH_3CCHNH
70	4	0	2		$C_2H_2N_2O^+$	C_3H_4O
58	0	0	1			
56	7	2	9		$C_3H_4O^+$	HNCO + HCN
55	100	47	100	11.7 ± 0.1	CH_3CCHNH^+	HNCO + CO
54	44	11	42	≈12.9	CH_2CCHNH^+	HNCO + CO + H
53	6	0	4			
52	14	0	2			
45	0	0	1			
44	6	0	9		CO_2 impurity	
43	4	0	2	11.9 ± 0.1	$HNCO^+$	C_4H_5NO
42	1	0	0			
41	<1	0	1			
40	6	0	7		$C_3H_4^+$	2HNCO
39	12	0	9	14.4 ± 0.1	$C_3H_3^+$	2HNCO + H
38	2	0	0			
37	2	0	0			
29	4	0	6			
28	59	6	67	13.6 ± 0.1	$HCNH^+$	(a)
27	36	0	11		$C_2H_3^+$ or HCN^+	
26	13	0	3		$C_2H_2^+$	HNCO + CO + H + HCNH (b)

(a) Four different pathways, with different initial neutral loss species. See text. (b) or could be HNCO + CO + CH_3N, the latter formed from the cyclic $m/z = 55$ by rupture of two bonds, but this is less evident than the pathway proposed in text.

20 eV electron impact mass spectrum (8 features) [32] as compared with our 20 eV photon impact mass spectrum (24 peaks, Table 3) illustrates well the difference in energy deposition with these two excitation sources, reflecting the fact that at 20 eV, electron impact is far from the Born approximation conditions [84] in which electron impact mimics photon impact excitation. Interestingly, the loss of HNCO from the parent ion is relatively more favored in the 20 eV electron impact as compared with the 20 eV photon impact case (see Table 3). This is consistent with the observation that HNCO loss corresponds to the lowest energy dissociative ionization process (AE = 10.7 eV, Table 3).

3.2.1. The thymine parent ion

For the parent ion, $m/z = 126$, we measured an ionization energy of 8.82 ± 0.03 eV (Fig. 6). In Table 4 this value is compared with those determined by various techniques. It is in excellent agreement with the only other value measured by photoionization mass spectrometry [67]. As in the case of adenine, an early measurement of thymine by electron impact [68] gives a value that is too high, but later measurements [69,70] give values much closer to our observed PIMS IE. The vertical IEs obtained by photoelectron spectroscopy peak measurements [23,31] are 200–380 meV above the adiabatic values determined by PIMS and electron impact measurements. This is of the same order of magnitude as the 240 meV predicted by a B1LYP functional [85] calculation [75], and 270 meV by a B3LYP functional calculation [86], for the difference between adiabatic and vertical IEs of thymine.

Using our measured adiabatic IE of thymine, and the known value of the heat of formation ΔH_f^0 (thymine) = −328.70 kJ/mol [78], we obtain a value of the heat of formation of the cation ΔH_f^0 (thymine cation) = 522.36 kJ/mol, which is very close to the preliminary value ΔH_f^{298} (thymine cation) = 520 kJ/mol given by Lias et al. [78], based on a quoted PES onset value of the IE = 8.8 eV. A direct comparison between the $m/z = 126$ ion yield curve and the HeI photoelectron spectrum of thymine measured by Urano et al. [24] revealed a few shoulders or apparent steps in the ion yield curve at energies close to those of several features in the photoelectron spectrum (Fig. 3(b)), but less marked than in the corresponding case of adenine. These features are related to the PES bands assigned to the π_1, n_1, π_2 and π_3 orbitals of thymine [24], as well as to some unassigned higher energy PES features. An inflection that we observe at ~11.7 eV in the parent ion yield curve has no obvious feature in the photoelectron spectra of thymine. One possibility is that this corresponds to an autoionization process in a Franck–Condon gap [87].

Table 4
Thymine ionization energy values[a]

Experimental method	Ionization energy (eV)	Reference and year
Photoion yield curve (PIMS)	8.82 ± 0.03	Present study
Electron impact ion yield curve	9.43 ± 0.10	[68] 1967
Photoelectron spectroscopy (PES)	9.14 ± 0.03 (vert)	[23] 1975
PES	9.02[b] (vert?)	[25] 1975
PIMS	8.87 ± 0.05	[67] 1976
Electron impact ion yield curve	8.95 ± 0.10	[69] 1976
PES	9.20[b] (vert)	[28] 1976
PES	9.18[b] (vert)	[24] 1989
Electron impact ion yield curve	9.15 ± 0.15	[70] 1996

[a] Adiabatic values unless otherwise stated.
[b] Uncertainty not reported.

At higher energies, there is a marked rise in the parent ion yield at about 16 eV, leading to a maximum at about 19.3 eV. Although the PES intensity drops markedly between 15 and 16 eV, in contrast to the parent ion yield curve, it shows, between 16 and 20 eV, a somewhat similar behaviour to the latter. This region of the PES has not been assigned but we note that there are similar features in the PES of pyrimidine in this energy region, for which molecular orbital assignments have been made [79].

Just as in the case of adenine, we compared the thymine parent ion yield curve with the optical absorption curve derived from 25 keV electron energy loss spectra of thin films of thymine [57] (Fig. 4(b)). Our parent ion yield curve has a plateau between 13 and 15.5 eV, followed by a rise to about 17.7 eV, continuing on to a peak at about 19 eV. In the thymine film spectrum, there are peaks reported to be at 14.4 ± 0.3 and 18.3 ± 0.3 eV [57]. The physical relation between these solid and gas phase features requires further investigation.

3.2.2. Thymine ion fragmentation

(α) *Reactions involving loss of HNCO and/or CO:* The principal fragmentation pathways of the thymine parent cation (species IV, see schematic representation Fig. 7) involve loss of HNCO (isocyanic acid). One unit loss gives rise to the $m/z = 83$ ion, whose AE = 10.7 eV:

$$C_5H_6N_2O_2^+ \ (m/z = 126) \rightarrow C_4H_5NO^+ \ (m/z = 83) + HNCO \ (m = 43) \qquad (14)$$

This ion is formed by Retro–Diels–Alder (RDA) reaction from the thymine parent cation, and involves the rupture of two bonds, N3–C4 and C2–N1, in the parent ion. The latter bond has been calculated to be much weakened in the cation as compared with neutral thymine [75]. The $m/z = 83$ fragment ion has been suggested to have the structure of species Va (Fig. 7) [38]. This is supported by recent calculations of the possible minimum energy structures and relative stabilities of $C_4H_5NO^+$ isomers [75]. We remark that the mass spectrum of ^{14}C2-thymine [34] retains the $m/z = 83$ peak, confirming that the ^{14}C2 atom has been eliminated in the HNCO loss molecule, as proposed in reaction (14).

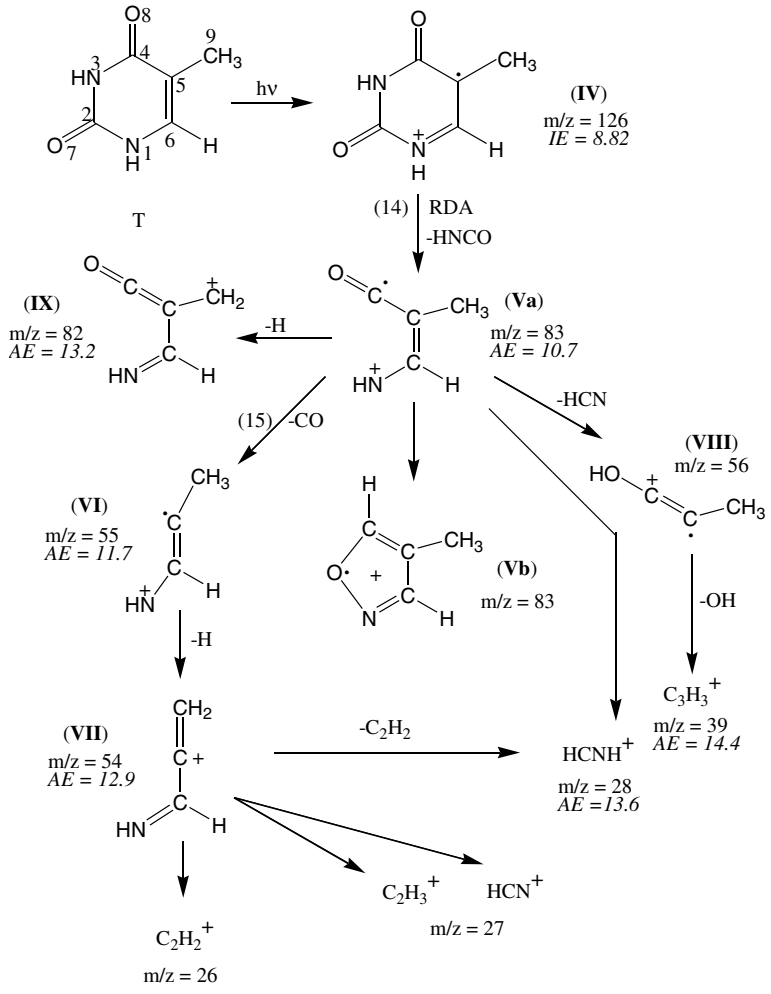

Fig. 7. Principal fragmentation decay routes of the thymine radical cation. Measured appearance energy values are given for each fragment (in eV, for uncertainties refer to Table 3). Roman and Arabic numerals correspond to species and reactions, respectively.

One possible evolution of the Va $C_4H_5NO^+$ ion that we considered is ring closure to form the 5-methyl-isoxazole cation. The heat of formation of the 5-methyl-isoxazole cation is $\Delta H_f = 931$ kJ/mol, obtained from the heat of formation of neutral 5-methyl isoxazole, $\Delta H_f = 34$ kJ/mol [65], and its adiabatic IE $= 9.3 \pm 0.1$ eV, which we determined from the published HeI photoelectron spectrum of Kobayashi et al. [88]. However, we find that the heat of formation of the observed $C_4H_5NO^+$ ion, $\Delta H_f(C_4H_5NO^+) = 806$ kJ/mol, based on its measured appearance energy, is considerably smaller than that of the 5-methyl isoxazole cation, which shows that the latter is not formed in our experiment. Another possibility is that the evolution is to the 4-methyl isoxazole cation (species Vb in Fig. 7), which is a δπ system. Thermochemical data on this species are not available. We note that the weak ion $m/z = 84$, observed in both the 20 and 70 eV electron impact mass spectra (Table 3), would correspond to the loss of NCO from IV.

The loss of two HNCO units gives rise to the $m/z = 40$ ion, assigned to CH_3–C≡CH^+. This can occur directly from parent ion via rupture of the two bonds, C4–C5 and, N1–C6. However, the calculations of Improta et al. [75] suggest that while the C4–C5 bond would be considerably weaker in the cation, the N1–C6 bond would be stronger. Formation of the $m/z = 40$ ion would be more complex, if it occurred via $m/z = 83$, since it would involve rupture of two further bonds in this intermediate ion to lose CO + NH.

Concerning the evolution of the $m/z = 83$ fragment ion, we note that it can go on to lose a CO molecule to form the most abundant ion in the mass spectrum, $m/z = 55$, whose AE = 11.7 eV.

$$C_4H_5NO^+ \ (m/z = 83) \rightarrow C_3H_5N^+ \ (m/z = 55) + CO \ (m = 28) \qquad (15)$$

This fragment ion, whose m/z value is, as expected, unchanged in the mass spectrum of ^{14}C2-thymine [34], has a proposed quasi-linear structure shown in Fig. 7 (species VI). Although this is the thermodynamically most favored structure, other isomers might be kinetically more accessible according to the calculations of Improta et al. [75].

Another possible assignment of $m/z = 55$ is to CH_3CCO^+ (methylketene ion which could eventually isomerize to $CH_2{=}CHCO^+$ or $HC{\equiv}CCH_2O^+$) that can be formed by rupture of the central carbon–carbon bond in $m/z = 83$. This corresponds to the charge switch of one of the reactions that can form $m/z = 28$ (see below). However, it is generally considered [38] that the $m/z = 55$ ion is indeed CH_3CCHNH^+, containing the methyl group and the atoms N1, C5 and C6.

The $m/z = 83$ ion can also lose a hydrogen atom, suggested to be from the methyl group [32], to give $m/z = 82$. It has been proposed [32] that further loss, of a CO group, is responsible for the formation of the strong $m/z = 54$ fragment ion $C_3H_4N^+$. However, our ion yield measurements show that the AE of $m/z = 54$ (~12.9 eV) is smaller than that of $m/z = 82$ (13.2 eV). Thus, there must exist some other mechanism of formation of the $m/z = 54$ ion at threshold. This is most probably loss of a hydrogen atom from the $m/z = 55$ species. It is of interest that the maximum in the $m/z = 55$ ion yield curve is at about 16 eV (Fig. 6) whereas it is at about 19 eV for the $m/z = 54$ ion, not far from the maximum in the parent ion curve (19.3 eV). The difference in energy is of the order of magnitude of the dissociation energy of a C–H bond. We remark that two different structures could exist for the $m/z = 54$ species, the quasi-linear species VII in Fig. 7, and a cyclic structure in which a methyl group is attached to a (H)CCN cyclic group [32].

(β) *Other important ions:* The weak $m/z = 43$ ion ($AE = 11.9 \pm 0.1$) eV, assigned to $HNCO^+$, could be the fragment ion formed in a reaction corresponding to a charge switch in the reaction (14) which leads to the formation of the $m/z = 83$ ion discussed above. We note that the shift of the $m/z = 43$ peak to $m/z = 45$ in the ^{14}C2-thymine mass spectrum published by Ulrich et al. [34] confirms our suggestion above that this ion is produced by a charge switch of reaction (14). The $m/z = 43$ ion is not observed in the 20 eV electron impact mass spectrum, although it is present in the 20 eV photon impact spectrum. This is consistent with the fact that the $m/z = 83$ ion is relatively much weaker in the 20 eV electron impact as compared with the photon impact mass spectrum (Table 3).

Following the Stevenson–Audier–Harrison (SAH) rule concerning the dissociation of odd electron ions [89], the fact that $m/z = 83$ has a smaller AE than $m/z = 43$ suggests that the $m = 83$ neutral species (C_4H_5NO) has a smaller IE than HNCO, whose $IE = 11.61 \pm 0.03$ eV [78]. This is certainly the case for the 5-methyl isoxazole form of C_4H_5NO, whose IE(v) = 9.61 eV [88] and whose IE(ad) we have determined as 9.3 ± 0.1 eV (see above). However, the C_4H_5NO product is not 5-methyl isoxazole since, from the 11.9 eV appearance energy of $m/z = 43$ and the heats of formation of thymine and of $HNCO^+$, we calculate the heat of formation of neutral C_4H_5NO to be −198 kJ/mol whereas, as mentioned above, the known heat of formation of 5-methyl isoxazole is 34.1 ± 0.75 kJ/mol [65]. Nor can C_4H_5NO be 3-methyl isoxazole, since the latter has $\Delta H_f = 35.6 \pm 0.67$ kJ/mol [65].

$m/z = 39$: The most probable assignment of the $m/z = 39$ ion is to $C_3H_3^+$, which could be formed by loss of a hydrogen atom from $C_3H_4^+$ ($m/z = 40$). The high AE = 14.4 eV of $m/z = 39$ is consistent with the energy expensive pathways suggested above for formation of its precursor ion, $m/z = 40$. Another possible formation pathway would be OH loss from $m/z = 56$ (species VIII in Fig. 7), whose formation is discussed below.

$m/z = 28$: The suggested linear structure of the $m/z = 54$ ion could give rise to formation of the $HCNH^+$ ($m/z = 28$) and $C_2H_2^+$ ($m/z = 26$) ions by rupture of the central carbon–carbon bond. The important $HCNH^+$ ion could also be formed by rupture of the central carbon–carbon bond in the $m/z = 82$ fragment ion (species IX in Fig. 7). Another mechanism involves direct formation of $HCNH^+$ from the parent ion, which requires rupture of two bonds, the C5–C6 double bond and the C2–N1 bond, both of which are calculated to be weaker in the cation [75]. We also note that from the structure of the $C_4H_5NO^+$ ion ($m/z = 83$, species Va) proposed above, it is possible, by rupture of the central carbon–carbon bond, to produce $HCNH^+$. This is pathway E of Rice et al. [32] in which there would be loss of the methylketene radical CH_3CCO. It is not clear as to whether this actually occurs since there is no mention of a metastable peak for this process. Thus we have suggested five different possible pathways for forming the $HCNH^+$ ion, via the respective precursors $m/z = 126$, 83, 82, 55 and 54, which in the latter three cases involves rupture of only one, carbon–carbon, bond. The AEs of the various fragment ions are consistent with all five pathways. From the profiles of their respective ion yield curves, it appears that the relative importance of these five pathways to forming the $HCNH^+$ ion is modified above 16 eV, since the 16 eV maximum in the ion yield curves of the $m/z = 55$ and 83 ions is at a much lower energy than the maxima in the other three precursor ion yield curves (Fig. 6).

A final remark concerning the $m/z = 28$ ion, assigned above to $HCNH^+$, is that it is unlikely to be CO^+ since CO has a quite high ionization energy (14.014 eV [65]), whereas the $m/z = 28$ ion has an AE = 13.6 eV, lower than IE(CO).

(γ) *Less intense fragment ion peaks (no AE measurements):* There is no initial loss of CO from the parent ion, since the $m/z = 98$ fragment ion is absent in the mass spectra. A weak ion is observed at $m/z = 97$, which is possibly $C_4H_3NO_2^+$, resulting from loss of NH_2CH. We have not yet discussed the very weakest ions observed in our mass spectrum of thymine, at $m/z = 71$,

70, 58, 56, 53, 52, 45, 41, 27: (Table 3). Of these, $m/z = 45$ and 58 were not observed in the mass spectrum of Rice et al. [32], although $m/z = 45$ is present in the mass spectrum of Ulrich et al. [34] and in that of the NIST [65].

$m/z = 70$, 71 and related species: We assign the $m/z = 71$ peak to $OCNHCO^+$, which could be formed from the parent ion by breaking of two bonds, C2–N1 and C4–C5. Both bonds are expected to be weaker in the cation from the calculations of Improta et al. [75]:

$$C_5H_6N_2O_2^+ \ (m/z = 126) \rightarrow OCNHCO^+ \ (m/z = 71) + CH_3CCHNH \ (m = 55) \quad (16)$$

This reaction also suggests that an alternative pathway for formation of the $m/z = 55$ ion would be a charge switch of reaction (16).

The $m/z = 70$ peak was assigned by Ulrich et al. [34] to $OCNCO^+$, based on a shift of two mass units in their mass spectra observed in a $^{14}C2$ study of thymine. We note that this fragment ion would not be formed by loss of a hydrogen atom from $m/z = 71$, since the latter peak is unchanged in the carbon isotope spectrum. However, an alternative assignment of $m/z = 70$, which we consider to be more probable, is to $C_2H_2N_2O^+$, whose structure would be that of the 1,2,5-oxadiazole cation. This could be formed from the parent cation by rupture of the C4–N3 and C5–C6 bonds and simultaneous formation of a bond between the C6 and N3 atoms. The resulting $m/z = 70$ ion would still be compatible with the mass spectrum of the $^{14}C2$ study of thymine by Ulrich et al. [34]. With this new assignment of the $m/z = 70$ ion, the neutral loss is of a species whose elemental formula is C_3H_4O and whose structure is that of methylketene.

$$C_5H_6N_2O_2^+ \ (m/z = 126) \rightarrow C_2H_2N_2O^+ \ (m/z = 70) + C_3H_4O \ (m = 56) \quad (17)$$

This assignment of $m/z = 70$ also makes possible a reasonable assignment of the $m/z = 56$ peak to the methylketene ion $C_3H_4O^+$ (an isomer of species VIII). The latter could be formed by a reaction corresponding to a charge switch of reaction (17). It is difficult to estimate whether this charge switch reaction is likely to occur, since although the ionization energy of methylketene is known, IE(v) = 8.95 eV [65], that of 1,2,5-oxadiazole has not been reported so far. The structure of the $m/z = 56$ ion could also correspond to a 1-methyl-2-hydroxyacetylene cation ($HO–C{=}CCH_3^+$), species VIII in Fig. 7), formed from ion Va ($m/z = 83$) by 1,5 H-shift with subsequent rupture of the central C–C bond. This reaction would most likely represent the unique HCN loss reaction for this nucleobase cation, in contrast, of course, to adenine, where multiple HCN loss processes occur. Isotopic studies are required to show whether this assignment of $m/z = 56$ is viable.

The weak peak at $m/z = 53^+$ is not assigned. The $m/z = 52$ ion is quite strong in the 70 eV electron impact mass spectrum, but absent in the 20 eV electron impact spectrum. This indicates, as do the intensities of some other relatively small fragment ions in the respective mass spectra, that they result from higher energy dissociative ionization processes. There are two assignments (HCN^+, $C_2H_3^+$) for the $m/z = 27$ ion. HCN^+ could be formed by loss of a hydrogen atom from $HCNH^+$. The formation of $C_2H_3^+$ is not easily rationalized. Isotopic labeling experiments are required to clarify the relative importance of these two $m/z = 27$ fragment ions.

3.3. Uracil: mass spectra and ion yield curves

Table 5 presents the relative intensities of the m/z peaks in our uracil mass spectrum, obtained at 20 eV photon excitation energy, and compares them with those of Rice et al. [32], measured with 70 eV electron impact, and with the 20 eV electron impact spectra of Hecht et al. [41] and of Rice et al. [32]. The appearance energies of the major m/z ions are listed, as measured from the onsets in the photoion yield curves (Fig. 8), and we give the neutral species which we consider to be formed by dissociative ionization of uracil, along with the observed m/z ions.

Our 20 eV photon impact mass spectrum of uracil and the 70 eV electron impact one of Rice et al. [32] are very similar, having essentially the same m/z features but with a few differences in their relative intensities. The $m/z = 42$ fragment ion peak is the strongest in both cases, as it is in the 70 eV electron impact mass spectrum reported by Brown et al. [39]. Several other electron impact mass spectra of uracil have been reported, having the same principal ions but with relative intensities different from those measured by Rice et al. [32]. In these mass spectra the parent peak at $m/z = 112$ is the most intense [34,38,40,65,90] and the intensities of the other principal peaks are in the m/z order $42 > 69 > 28$ [34,40] or $69 > 42 > 28$ [38,65,90,91]. As mentioned earlier, the differences between the 70 eV electron impact spectra are most probably due to differences in the ion optics and ion residence times.

The 20 eV electron impact mass spectra of uracil obtained by Rice et al. [32] and by Hecht et al. [41] also have the parent peak as its most intense ion, with the other principal peaks being $m/z = 69$, 42 and 28. The much smaller number of m/z peaks in the 20 eV electron impact mass spectrum of Rice et al. [32] (10 features) of uracil as compared to our 20 eV photon impact mass spectrum (Table 5) can here too be understood, as in the similar case of thymine, as being due to a different energy deposition with these two excitation sources, since at 20 eV electron impact the Born approximation conditions [84] under which electron impact mimics photon impact excitation is not operative at this low electron excitation energy. However, we note that the

Table 5
Electron impact [32,41] and photon impact mass spectra and photoion appearance energies: Uracil $m = 112$ ($C_4H_4N_2O_2$)

m/z	Electron impact 70 eV relative intensity	Electron impact 20 eV relative intensity[a]	Photon impact 20 eV relative intensity	Photon impact appearance energy (AE, eV)	Ion elemental formula	Neutral loss
112	78	100(100)	63	9.15 ± 0.03	$C_4H_4N_2O_2^+$	
96	2	0(0)	1		$C_4H_4N_2O^+$	O
95	0	<1(2)	0			
77	0	<1(0)	0			
70	7	5(5)	4		$C_3H_4NO^+$	NCO
69	63	69(66)	52	10.95 ± 0.05	$C_3H_3NO^+$	HNCO
68	33	15(5)	33	13.40 ± 0.05	$C_3H_2NO^+$	HNCO + H
67	1	<1(0)	0			
56	3	<1(0)	3			
53	4	<1(0)	1			
52	1	<1(0)	1			
51	1	<1(0)	0			
44	8	4(1)	4			
43	15	6(1)	10	13.6 ± 0.2	$HNCO^+$	C_3H_3NO
42	100	59(21)	100	13.25 ± 0.05	$C_2H_2O^+$	HNCO + HCN
41	48	21(8)	50	12.95 ± 0.05	$HCCHNH^+$ and/or $HCCO^+$	HCNO + CO and/or HNCO + HCN + H
40	57	21(0)	25	14.06 ± 0.10	$C_2H_2N^+$	HNCO + H + CO
39	15	5(0)	2			
38	7	2(0)	0			
32	0	2(0)	0			
31	0	<1(0)	0			
29	1	2(0)	3		NH_2CH^+ or HCO^+	
28	78	74(10)	86	13.75 ± 0.05	$HCNH^+$	HNCO + HCCO
27	2	3(0)	4		HCN^+	HNCO + HCCO + H
26	4	4(0)	5	≈15 eV	$C_2H_2^+$	2HNCO
18	n.m.[b]	n.m.	4		H_2O^+	Also observed in NIST
17	n.m.	n.m.	1		NH_3^+	Also observed in NIST
14	n.m.	n.m.	3		N^+	Also observed in NIST

[a] Data from the 20 eV electron impact mass spectra of Hecht et al. [41] and, in parentheses, of Rice et al. [32].
[b] n.m. = not measured.

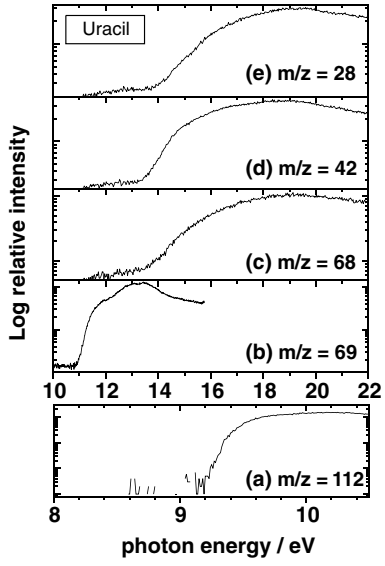

Fig. 8. Selected ion yield curves of uracil. The $m/z = 112$ ion yield curve has been measured using an MgF_2 cut-off filter.

reported 20 eV electron impact mass spectrum of uracil, by Hecht et al. [41] (Table 5), contains many more, mainly very weak, features, and that the principal peak intensities are often much closer to those observed in the 70 eV electron impact mass spectrum. It would thus appear that the ion residence time was much longer in the 20 eV electron impact experiments of Hecht et al. [41] than in those of Rice et al. [32].

Coupier et al. [91] recently measured both proton (20–150 keV) impact and electron (200 eV) impact mass spectra of uracil. They observed the same principal fragment ions as in our 20 eV photon impact study, but discussed only four of the fragment ions, $m/z = 69$, 42, 29 and 28, giving the latter three different molecular ion assignments than ours, as discussed later. Especially in the proton impact spectrum, they also observed a very large number of other fragment ions, this being due, no doubt, to the increased energy deposition with respect to our case and to that of 70 eV electron impact. In the proton impact study, the order of the principal

ion intensities was $m/z = 112 = 42 > 28 > 69$, whereas in the 200 eV electron impact mass spectrum it was $m/z = 28 > 42 > 69 > 112$.

3.3.1. The uracil parent ion

For the uracil ion $C_4H_4N_2O_2^+$, $m/z = 112$, we obtained an ionization energy of 9.15 ± 0.03 eV from the parent ion yield curve, measured using an MgF_2 filter (Fig. 8(a)). This value is a little smaller than the IE $= 9.32 \pm 0.05$ eV obtained with the only other reported measurement by photoionization mass spectrometry [67] Table 6. Early measurements of uracil by electron impact gave IE values that are rather high [68,92], but a later measurement [69] is much closer to our PIMS value. A recent electron impact measurement [90] also gave a value, IE $= 9.59 \pm 0.08$ eV, considerably higher than our PIMS value, but similar to the vertical IEs of uracil obtained by photoelectron spectroscopy peak measurements [23,27–29,93]. The PES IE(vert) values fall in the range 9.50–9.68 eV, i.e., 350–530 meV above the adiabatic value determined by our PIMS measurement. The calculations of IE(ad) and IE(vert) reported for this RNA base by Wetmore et al. [94] give values IE(ad) = 9.21 eV and IE(vert) = 9.47 eV, a difference of 260 meV.

As in the case of adenine and thymine, a direct comparison between the $m/z = 112$ ion yield curve and the HeI photoelectron spectrum of uracil [24] revealed features in the ion yield curve that can be correlated with features in the photoelectron spectrum (see Fig. 3(c)). Also, there is a general similarity in the parent ion yield curves of the two related nucleobases uracil and thymine. In particular, in both cases there is a marked rise

Table 6
Uracil ionization energy values[a]

Experimental method	Ionization energy (eV)	Reference and year
Photoion yield curve (PIMS)	9.15 ± 0.03	Present study
Electron impact ion yield curve	9.82 ± 0.10	[68] 1967
Electron impact ion yield curve	9.53 ± 0.02	[92] 1971
Photoelectron spectroscopy (PES)	9.59 ± 0.03 (vert)	[93] 1974
PES	9.50 ± 0.03 (vert)	[23] 1975
PES	9.45[b] (vert)	[25] 1975
PES	9.60[b] (vert)	[28] 1976
PIMS	9.32 ± 0.05	[67] 1976
Electron impact ion yield curve	9.35 ± 0.10	[69] 1976
PES	9.68[b] (vert)	[27] 1980
PES	9.53[b]	[29] 1996
Electron impact ion yield curve	9.59 ± 0.08 (vert)	[90] 2004

[a] Adiabatic values unless otherwise stated.
[b] Uncertainty not reported.

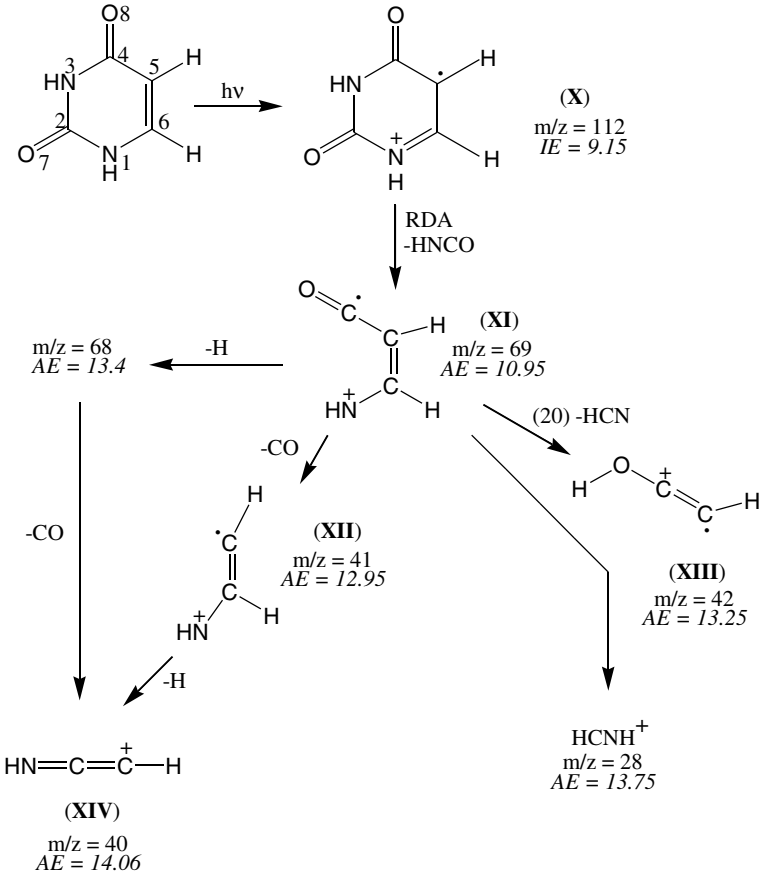

Fig. 9. Principal fragmentation decay routes of the uracil radical cation. Measured appearance energy values are given for each fragment (in eV, for uncertainties refer to Table 5). Roman and Arabic numerals correspond to species and reactions, respectively.

in the parent ion yield at about 16 eV, leading to a maximum in the 19.3–19.5 eV region.

Using our measured adiabatic IE of uracil, and the known value of the heat of formation $\Delta H_f^0(\text{uracil}) = -303 \pm 2$ kJ/mol [78], we obtain a value of the heat of formation of the cation $\Delta H_f^0(\text{uracil cation}) = 580 \pm 5$ kJ/mol, in agreement with the preliminary value 585 kJ/mol given by Lias et al. [78], based on the onset of a photoelectron spectral band.

3.3.2. Uracil ion fragmentation

(α) *Reactions involving loss of HNCO and CO*: The principal fragmentation pathways of the uracil parent cation (species X, Fig. 9) involve loss of HNCO by RDA reaction as in the case of thymine. This gives rise to the $m/z = 69$ ion, $C_3H_3NO^+$, whose AE = 10.95 ± 0.05 eV. This ion has been suggested [38] to have the structure given in Fig. 9 (species XI). In their electron impact ionization study of uracil, Denifl et al. [90] measured AE = 10.89 ± 0.07 eV for the appearance of the $m/z = 69$ ion, which is close to our photon impact value. They, as well as Coupier et al. [91], also assigned it to $C_3H_3NO^+$, i.e., the "X-HNCO" ion, but did not discuss its structure. The formation of species XI, by loss of HNCO involves rupture of the N3–C4 and C2–N1 bonds.

The charge switch reaction:

$$C_4H_4N_2O_2^+ \rightarrow HNCO^+ \ (m/z = 43) + C_3H_3NO \ (m = 69) \quad (18)$$

gives rise to the $m/z = 43$ ion, $HNCO^+$, whose AE = 13.6 ± 0.2 eV in our PIMS measurement and is reported to be 13.36 ± 0.30 eV in electron impact measurements [90]. The AE of $HNCO^+$ is much greater than the AE = 10.95 eV of $C_3H_3NO^+$. This suggests, from the SAH rule [89], that IE (C_3H_3NO) is smaller than the IE of HNCO (11.61 ± 0.03 eV [78]). The two most likely candidates for C_3H_3NO are in concordance with this suggestion: isoxazole (IE = 9.942 eV [95]) and oxazole (IE = 9.6 eV [96]). Heat of formation calculations favor oxazole.

The $m/z = 69$ fragment ion can further fragment by a number of different pathways. Many of these pathways in uracil (U) are similar to corresponding pathways in the fragmentation of the $m/z = 83$ ion of thymine (T), but their relative importance is very different in the two cases, as can be seen by a comparison of the relative intensities of the precursor ion (m/z(U) = 69, m/z(T) = 83), and relevant daughter ion in Tables 3 and 5. We will discuss these various pathways in turn.

Whereas in m/z(T) = 83, loss of a CO molecule forms $m/z = 55$, the most abundant ion in the thymine mass spectrum, in uracil, for m/z(U) = 69, the corresponding CO loss gives rise to the $m/z = 41$ fragment ion, assigned to $HC{=}CHNH^+$ (species XII in Fig. 9) which, although intense, is not the major fragment ion in the uracil mass spectrum.

$$C_3H_3NO^+ \ (m/z = 69) \rightarrow HC{=}CHNH^+ \ (m/z = 41) + CO \ (m = 28) \quad (19)$$

This pathway has been confirmed by the observation of a satisfactory metastable peak in the electron impact mass spectrum of Rice et al. [32]. Other possible isomers of $C_2H_3N^+$ are the species $HN{=}C{-}CH_2^+$, formed by H-shift from XII, as well as the azirinium radical cation and the 2H-azirine cation ring species, the formation of both of which would involve complicated rearrangements.

We find that the $m/z = 41$ ion has an AE = 12.95 ± 0.05 eV, i.e., 3.80 eV above the IE of uracil, whereas the m/z(T) = 55 ion appears at 2.88 eV above the IE of thymine. We note that in their electron impact study of uracil, Denifl et al. [90] observed AE = 13.32 ± 0.18 eV for the $m/z = 41$ ion, somewhat higher than our PIMS value; however, the difference between this value and their measured IE = 9.59 ± 0.08 eV for the parent ion is 3.73 eV, similar to our PIMS value. That these uracil values are greater than the 2.88 eV observed for thymine indicates the greater difficulty of CO loss in the uracil case with respect to the precursor ion in thymine. In the latter, with respect to uracil, the presence of the methyl group no doubt weakens the carbon–carbon bond to which the oxygen atom is attached, via hyperconjugation that affects the π electron distribution. We note that there is no initial loss of CO from the parent ion, since the $m/z = 84$ fragment ion is absent in the mass spectrum of uracil.

(β) *Other important ions:* We now discuss the most intense fragment ion, $m/z = 42$. This is assigned to the $HC{=}COH^+$ ion (species XIII), formed by 1,5 H-shift and subsequent loss of HCN from the $m/z = 69$ precursor ion (reaction (20)). We note that loss of HNC from XIII could give rise to the isomer $H_2C{=}C{=}O^+$, the ketene radical cation. The structure of ion $m/z = 42$ remains to be further investigated

$$C_3H_3NO^+ \ (m/z = 69) \rightarrow HC{=}COH^+ \ (m/z = 42) + HCN \ (m = 27) \quad (20)$$

The assignment of $m/z = 42$ to $HC{=}COH^+$ is consistent with the fragmentation patterns from electron impact mass spectra of at least four 2,4-dioxypyrimidenes [32,38], whose structures are related to uracil. We remark that the electron impact measurement of Denifl et al. [90] gave AE = 13.41 ± 0.10 eV, in reasonable agreement with our value AE = 13.25 ± 0.05 eV, for m/z(U) = 42. These authors, as well as Coupier et al. [91], assigned $m/z = 42$ to the OCN^+ ion. However, formation of a OCN^+ fragment ion directly from the parent ion would involve rupture of three bonds. It would also involve a very complex bond rupture and reorganization process if the precursor was the $m/z = 69$ ion represented in Fig. 9. We prefer our assignment of the $m/z = 42$ peak to the $HC{=}COH^+$ ion (or its isomer

$H_2C{=}C{=}O^+$), whose formation is mechanistically more reasonable.

The incorrect assignment of the $m/z = 42$ ion to OCN^+ has further implications. Feil et al. [97] have very recently measured the absolute value of the partial cross-section for formation of this cation in electron excitation of uracil, and then used this cross-section, which they assumed was that of the OCN^+ ion, in conjunction with the known sensitivity ratio for detection of positive and negative ions of the same species, to determine the dissociative attachment cross-section for formation of the OCN^- anion from uracil. The value they obtained was smaller by an order of magnitude than that previously obtained with uracil by simple normalization with the cross-section for dissociative electron detachment in CCl_4 [98]. Although it is very possible that the $m/z = 42$ anion formed by dissociative electron detachment in uracil is indeed OCN^-, it appears unlikely that the $m/z = 42$ cation is OCN^+. We suggest that incorrect assignment of the $m/z = 42$ cation to OCN^+ is in part responsible for the discrepancy between the two OCN^- cross-section values.

Another fragmentation pathway with $m/z = 69$ as precursor ion leads, by rupture of the central carbon–carbon bond, to formation of $HCNH^+$ ($m/z = 28$), $AE = 13.75 \pm 0.05$ eV, by loss of the ketene radical HC=C=O.

$$C_3H_3NO^+ \ (m/z = 69) \rightarrow HCNH^+ \ (m/z = 28) + HC{=}C{=}O \ (m = 41) \quad (21)$$

It is not clear as to whether this actually occurs since there is no mention of a metastable peak for this process in electron impact experiments [32]. We further remark that Coupier et al. [91] assign the $m/z = 28$ ion to CO^+ (see also [90]) but this is very unlikely, for reasons similar to those discussed previously for the analogous case in thymine. Denifl et al. [90] measure $AE = 13.83 \pm 0.39$ eV for $m/z = 28$, in good agreement with our PIMS value.

We note that the charge switch ion $HC{=}C{=}O^+$ ($m/z = 41$) to reaction (21) has the same m/z as $HC{=}CHNH^+$, $AE = 12.95$ eV, discussed above. Both ion products are suggested by the fragmentation schemes of Rice et al. [32]. The respective IEs of the HC=C=O radical (~9.5 eV [78]) and HC=CHNH (10.1–12.2 eV, according to the structure of this ion [65]) suggest that $HC{=}C{=}O^+$ could be a significant contributor to the $m/z = 41$ peak.

The $m/z = 69$ ion can also lose a hydrogen atom to give $m/z = 68$, which is a strong ion, whose $AE = 13.40 \pm 0.05$ eV. The electron impact measurement, $AE = 12.75 \pm 0.66$ eV, is not inconsistent with our PIMS value, given the large uncertainty in the electron impact value. It has been proposed [32] that the fairly strong $m/z = 40$ fragment ion (species XIV in Fig. 9) can be formed via two pathways: (i) loss of a CO group from $m/z = 69$, (species XI) followed by loss of a hydrogen atom, or (ii) loss of H from XI followed by loss of CO. Both pathways are indicated in Fig. 9. Our ion yield measurements show that the AE of $m/z = 40$ (14.06 eV) is much greater than that of $m/z = 69$ (10.95 eV) and of the AE of the respective intermediate ions $m/z = 41$ and $m/z = 68$. This is consistent with the $m/z = 40$ ion resulting from three stages of fragmentation.

On the basis of the corresponding studies on thymine, it is possible to propose two different structures for a $C_2H_2N^+$ assignment of the $m/z = 40$ species, a quasi-linear $HN{=}C{=}CH^+$ (species XIV in Fig. 9) and a cyclic structure in which a nitrogen atom is attached to two linked CH groups. However, in contrast to the case of thymine, where the corresponding $m/z(T) = 54$ ion is considered to have the structure $H_2C{=}C{=}CHNH^+$ (species VII), from which formation of the $HCNH^+$ ($m/z = 28$) ion can occur by rupture of the central carbon–carbon bond, the corresponding precursor ion in uracil, $HN{=}C{=}CH^+$ [32], does not have a suitable structure for easy formation of HCNH+.

We must remember that there is also a totally different assignment possible for the $m/z = 40$ ion, i.e., CCO^+, formed by loss of a hydrogen atom from a $HC{=}C{=}O^+$ ($m/z = 41$) precursor that could be formed as discussed above. However, Rice et al. [32] affirm that the only ion observed at $m/z = 40$ is $C_2H_2N^+$. Isotopic labeling studies would be useful to clarify this assertion.

Another mechanism for producing $HCNH^+$ involves direct formation from the parent ion, which requires rupture of two bonds, the C5–C6 double bond and the C2–N1 bond (Fig. 1), similar to the case of thymine:

$$C_4H_4N_2O_2^+ \ (m/z = 112) \rightarrow HCNH^+ \ (m/z = 28) + C_3H_2NO_2 \ (m = 84) \quad (22)$$

In contrast to thymine, for which we have suggested five different possible pathways for forming the $HCNH^+$ ion, in the case of uracil (U) there appear to be only two viable pathways to the formation of $HCNH^+$, via reactions (21) and (22), respectively. The $AE = 13.75$ eV of $m/z(U) = 28$ and the AEs of the precursor ions (10.95 and 9.15 eV, respectively) are consistent with these two pathways. We note, however, that the intensity of the $m/z = 69$ ion decreases rapidly above 13.7 eV which is close to the onset of the $m/z = 28$ eV ion yield curve. This suggests that both pathways to formation of $HCNH^+$ are operative, weakly from the parent ion precursor, and strongly from the $m/z = 69$ precursor.

(γ) *Less intense fragment ion peaks (no AE measurements):* The other fragment ion peaks in Table 5 belong to minor ions, some of which are associated with high energy processes.

$m/z = 96$: This weak ion is assigned to $C_4H_4N_2O^+$ corresponding to loss of a single oxygen atom from

the parent ion. This could result from cleavage of the C4–O4 bond or the C2–O2 bond. We note that the 20 eV electron impact mass spectra contain a peak at $m/z = 95$ but not at $m/z = 96$, whereas the 70 eV electron impact mass spectra, like our 20 eV photon impact spectrum, possess a peak at $m/z = 96$ but not at $m/z = 95$. This requires further investigation.

We note that the weak ion $m/z = 70$ corresponds to the (U-NCO) cation.

$m/z = 29$, 27, 26: Coupier et al. [91] assign the $m/z = 29$ ion to HCO^+. An alternative assignment could be to the NH_2CH^+ ion. The $m/z = 27$ ion is assigned to HCN^+ but it is too weak for measurement of its appearance energy in our PIMS study. An electron impact measurement gave $AE = 14.77 \pm 0.92$ eV [90] for this ion. We assign the $m/z = 26$ ion to $C_2H_2^+$, formed via loss of 2 HNCO molecules directly from the parent ion by rupture of two bonds, C4–C5 and C6–N1. Ion yield measurement of this very weak ion at BESSY II showed that its AE is approximately 15 eV.

$m/z = 18$, 17 and 14: The peaks at $m/z = 18$, 17 and 14 in our 20 eV photon impact mass spectrum are below the lower mass limit ($m/z = 20$) reported in many electron impact studies [32,34,38–41]. However, these peaks can be seen in the NIST mass spectrum [65], in the proton and electron impact mass spectra [91] spectra, and in a 120 eV electron impact mass spectrum [97]. We consider these peaks to correspond, respectively, to H_2O^+, NH_3^+ and N^+ ions. The ratio of intensities of peaks $m/z = 18$ and 17 is the same in our 20 eV photon impact mass spectrum and in the NIST electron impact mass spectrum, whereas our $m/z = 14$ signal is relatively about twice as strong as that in the NIST spectrum. The existence of the $m/z = 14$ ion, assigned to N^+, lends credence to the assignment of $m/z = 17$ to NH_3^+ rather than to an OH^+ ion, which could occur, with about the same relative intensity to $m/z = 18$, from a water impurity [89].

4. Conclusion

In this photoionization mass spectrometry study of adenine, thymine and uracil, we used synchrotron radiation in the 6–22 eV photon energy region to investigate VUV-induced degradation pathways of these three nucleic acid bases in the gas phase. Photon impact mass spectra and photoion yields as a function of excitation energy were measured, virtually for the first time for these important biological molecules. The measurements provided more accurate values than previously reported for the adiabatic IEs of these nucleobases. These values are important for the interpretation of charge transfer phenomena in DNA and RNA.

We compared our 20 eV photoion mass spectra with 20 and 70 eV electron impact (and 200 eV electron and high energy proton impact in uracil) mass spectra. The existence of many metastable dissociation reactions, as seen in the electron impact studies, makes the number of m/z peaks and their relative intensities dependent on ion source residence time, field-free region characteristics and applied potentials in the ion optics. Particularly interesting is the comparison between 20 eV photon impact and 20 eV electron impact mass spectra for thymine and uracil, illustrating great differences in energy deposition due, in part, to the non-validity of the first Born approximation for low energy electrons.

The assignment of the m/z peaks in our photon impact mass spectra and analyses of fragment ion formation pathways have been considerably assisted by data published on the electron impact mass spectra of these nucleobases. In our work, the photoion appearance energies are reported for the first time. AE values enabled heats of formation of parent and some fragment ions to be revised or determined. Thermochemical data, coupled with the observed AEs, were also useful in clarifying dissociative ionization pathways many of which were first proposed by Rice and Dudek [32,33]. Our study has enabled us to refine these pathways, evaluate the relative importance of competitive processes in some cases and propose pathways that were not previously suggested.

For the purine, adenine, the ion fragmentation is mainly governed by successive loss of HCN units. The two pyrimidines, thymine and uracil, have similar dissociation pathways, with main neutral loss pathways which involve HNCO and CO and, in uracil, HCN. However, there are some significant differences due to hyperconjugation properties of the methyl group in thymine so that the relative importance of analogous reactions differs markedly, in some cases, between thymine and uracil. The astrophysically important fragment ion $HCNH^+$ can be formed by several fragmentation pathways in all three nucleobases. The relative importance of competitive fragmentation processes was determined in some cases.

Further concerning the astrophysical implications of our study, we note that the three nucleobases would be easily photodissociated in HI regions of the interstellar medium since they exhibit fragmentation appearance energies well below 13.6 eV. Thus their observation in the interstellar medium calls for study of regions of radiation protection (dark clouds) or regions where nucleobase production could successfully outweigh destruction. This is confirmed by the analogous case of the amino acid glycine which has very recently been reported to have been observed by radioastronomy in hot molecular core regions, where the visual extinction is very large, thus providing radiation protection [89,99]. The existence of nucleobases in meteorites and micrometeorites also implies that their formation and survival occurs in conditions of efficient VUV radiation shielding

as also implied by hydrogen lamp irradiation of nucleobases in low temperature matrices [100].

Acknowledgments

We thank Jean-Louis Chotin for technical assistance during BESSY runs. Support from the CNRS Groupe de Recherche "GDR Exobiologie" and from the CNES convention with INSU is gratefully acknowledged. We thank BESSY for use of its facilities in supporting the experimental studies under EC contract I 3 RII 3-CT-2004-506008. H.B. thanks the "Fonds des Chemischen Industrie" for financial support.

References

[1] A. Brack (Ed.), The Molecular Origins of Life, Cambridge University Press, Cambridge, UK, 1998.
[2] P.G. Stocks, A.W. Schwartz, Nature 282 (1979) 709.
[3] P.G. Stocks, A.W. Schwartz, Geochim. Cosmochim. Acta 45 (1981) 563.
[4] L.-L. Hua, K. Kobayashi, E.-I. Ochiai, C.W. Gerke, K.O. Gerhardt, C. Ponnamperuma, OLEB 16 (1986) 226.
[5] A. Shimoyama, S. Hagishita, K. Harada, Geochem. J. 24 (1990) 343.
[6] S. Chakrabati, S.K. Chakrabarti, Astron. Astrophys. 354 (2000) L6.
[7] I.W.M. Smith, D. Talbi, E. Herbst, Astron. Astrophys. 369 (2001) 611.
[8] J. Kissel, F.R. Krueger, Nature 326 (1987) 755.
[9] R.D. Brown, P.D. Godfrey, D. McNaughton, A.P. Pierlot, Chem. Phys. Lett. 156 (1989) 61.
[10] R.D. Brown, P.D. Godfrey, D. McNaughton, A.P. Pierlot, J. Chem. Soc. Chem. Commun. (1989) 37.
[11] R.D. Brown, P.D. Godfrey, D. McNaughton, A.P. Pierlot, J. Am. Chem. Soc. 110 (1988) 2329.
[12] P. Colarusso, K.-Q. Zhang, B. Guo, P.F. Bernath, Chem. Phys. Lett. 269 (1997) 39.
[13] M. Graindourze, J. Smets, T. Zeegers-Huyskens, G. Maes, J. Mol. Struct. 222 (1990) 345.
[14] A Yu Ivanov, A.M. Plokhotnichenko, E.D. Radchenko, G.G. Sheina, Yu.P. Blagoi, J. Mol. Struct. 372 (1995) 91.
[15] M.J. Nowak, J. Mol. Struct. 193 (1989) 35.
[16] M.J. Nowak, L. Lapinski, J. Kwiatkowski, J. Leszcynski, J. Phys. Chem. 100 (1996) 3527.
[17] L.B. Clark, G.G. Peschel, I. Tinoco Jr., J. Phys. Chem. 69 (1965) 3615.
[18] D.C. Lührs, J. Viallon, I. Fischer, Phys. Chem. Chem. Phys. 3 (2001) 1827.
[19] Chr. Plützer, E. Nir, M.S. de Vries, K. Kleinermanns, Phys. Chem. Chem. Phys. 3 (2001) 5466.
[20] M. Fujii, T. Tamura, N. Mikami, M. Ito, Chem. Phys. Lett. 126 (1986) 583.
[21] N.J. Kim, G. Jeong, Y.S. Kim, J. Sung, S.K. Kim, J. Chem. Phys. 113 (2000) 10052.
[22] K. Varmuza, W. Werther, F.R. Krueger, J. Kissel, E.R. Schmid, Int. J. Mass Spectrom. 189 (1999) 79.
[23] N.S. Hush, A.S. Cheung, Chem. Phys. Lett. 34 (1975) 11.
[24] S. Urano, X. Yang, P.R. LeBreton, J. Mol. Struct. 214 (1989) 315.
[25] G. Lauer, W. Schäfer, A. Schweig, Tetrahedron Lett. 45 (1975) 3939.
[26] C. Yu, T.J. O'Donnell, P.R. LeBreton, J. Phys. Chem. 85 (1981) 3851.
[27] M.H. Palmer, I. Simpson, R.J. Platenkamp, J. Mol. Struct. 66 (1980) 243.
[28] D. Dougherty, K. Wittel, J. Meeks, S.P. McGlynn, J. Am. Chem. Soc. 98 (1976) 3817.
[29] M. Kubota, T. Kobayashi, J. Electr. Spectrosc. Rel. Phenom. 82 (1996) 61.
[30] S. Peng, A. Padva, P.R. LeBreton, Proc. Natl. Acad. Sci. USA 73 (1976) 2966.
[31] J. Lin, C. Yu, S. Peng, I. Akiyama, K. Li, Li. Kao Lee, P.R. LeBreton, J. Am. Chem. Soc. 102 (1980) 4627.
[32] J.M. Rice, G.O. Dudek, M. Barber, J. Am. Chem. Soc. 87 (1965) 4569.
[33] J.M. Rice, G.O. Dudek, J. Am. Chem. Soc. 89 (1967) 2719.
[34] J. Ulrich, R. Teoule, R. Massot, A. Cornu, Org. Mass Spectrom. 2 (1969) 1183.
[35] J.L. Occolowitz, Chem. Commun. (1968) 1226.
[36] M.G. Barrio, D.I.C. Scopes, J.B. Holtwick, N.J. Leonard, Proc. Natl. Acad. Sci. USA 78 (1981) 3986.
[37] S.K. Sethi, S.P. Gupta, E.E. Jenkins, C.W. Whitehead, L.B. Townsend, J.A. McCloskey, J. Am. Chem. Soc. 104 (1982) 3349.
[38] J.A. McCloskey, in: P.O.P. TS'O (Ed.), Basic Principles in Nucleic Acid Chemistry, vol. I, Academic Press, New York, 1974, p. 209.
[39] E.G. Brown, B.S. Mangat, Biochim. Biophys. Acta 177 (1969) 427.
[40] K.C. Smith, R.T. Aplin, Biochemistry 5 (1966) 2125.
[41] S.M. Hecht, A.S. Gupta, N.J. Leonard, Biochim. Biophys. Acta 182 (1969) 444.
[42] S. Gohlke, E. Illenberger, Europhys. News 33 (2002) 207.
[43] R. Abouaf, J. Pommier, H. Dunet, Int. J. Mass Spectrom. 226 (2003) 397.
[44] J. deVries, R. Hoekstra, R. Morgenstern, T. Schlathölter, Phys. Rev. Lett. 91 (2003) 053401.
[45] L.P. Candeias, S. Steenken, J. Am. Chem. Soc. 114 (1992) 699.
[46] L.H. Seah, L.A. Burgoyne, J. Photochem. Photobiol. B 61 (2001) 10.
[47] E.M. Conwell, D.M. Basko, J. Am. Chem. Soc. 123 (2001) 11441.
[48] A. Heller, Faraday Discuss 116 (2000) 1.
[49] M. Bixon, J. Jortner, J. Am. Chem. Soc. 123 (2001) 12556.
[50] F. Jolibois, J. Cadet, A. Grand, R. Subra, V. Barone, N. Rega, J. Am. Chem. Soc. 120 (1998) 1864.
[51] P.-W. Hou, R.P. Rampling, J. Appl. Phys. 47 (1976) 4572.
[52] L.C. Emerson, M.W. Williams, I'lan. Tang, R.N. Hamm, E.T. Arakawa, Radiat. Res. 63 (1975) 235.
[53] I.P. Vinogradov, V.V. Zemskikh, N. Ya Daononova, Opt. Spectrosc. 36 (1974) 344.
[54] T. Yamada, H. Fukutome, Biopolymers 6 (1968) 43.
[55] A. Pinchuk, J. Quant. Spectrosc. Radiat. Transfer 85 (2004) 211.
[56] R. Abouaf, J. Pommier, H. Dunet, Chem. Phys. Lett. 381 (2003) 486.
[57] M. Isaacson, J. Chem. Phys. 56 (1972) 1803.
[58] E.T. Arakawa, L.C. Emerson, S.I. Juan, J.C. Ashley, M.W. Williams, Photochem. Photobiol. 44 (1986) 349.
[59] T. Inagaki, A. Ito, K. Hieda, T. Ito, Photochem. Photobiol. 44 (1986) 303.
[60] H.W. Jochims, E. Rühl, H. Baumgärtel, S. Tobita, S. Leach, Int. J. Mass Spectrom. Ion Processes 167/168 (1997) 35.
[61] C. Chyba, C. Sagan, Nature 355 (1992) 125.

[62] M. Schwell, F. Dulieu, S. Leach, in: Proceedings of the First European Workshop on Exo-/Astro-Biology ESA 29-496, 2001, p. 133.
[63] M. Schwell, F. Dulieu, S. Leach, Astrobiology 1 (2001) 210.
[64] M. Schwell, F. Dulieu, C. Gée, H.-W. Jochims, J.-L. Chotin, H. Baumgärtel, S. Leach, Chem. Phys. 260 (2000) 261.
[65] NIST Chemistry WebBook. Available from: <http://webbook.nist.gov>.
[66] S. Leach, Z. Phys. Chem. 195 (1996) 15.
[67] V.M. Orlov, A.N. Smirnov, Ya.M. Varshavsky, Tetrahedron Lett. 48 (1976) 4377.
[68] C. Lifschitz, E.D. Bergmann, B. Pullman, Tetrahedron Lett. 46 (1967) 4583.
[69] B.I. Verkin, L.F. Sukodub, I.K. Yanson, Dokl. Akad. Nauk SSSR 228 (1976) 1452.
[70] S.K. Kim, W. Lee, D.R. Herschbach, J. Phys. Chem. 100 (1996) 7933.
[71] Chr. Plützer, K. Kleinermanns, Phys. Chem. Chem. Phys. 4 (2002) 4877.
[72] C.T. Hwang, C.L. Stumpf, Y.-Q. Yu, H.I. Kenttämaa, Int. J. Mass Spectrom. 182/183 (1999) 253.
[73] A.-O. Colson, B. Besler, D.M. Close, M.D. Sevilla, J. Phys. Chem. 96 (1992) 661.
[74] S.D. Wetmore, R.J. Boyd, L.A. Eriksson, J. Phys. Chem. B 102 (1998) 10602.
[75] R. Improta, G. Scalmani, V. Barone, Int. J. Mass Spectrom. 201 (2000) 321.
[76] J. Reynisson, S. Steenken, PCCP 4 (2002) 527.
[77] D.L. Hildebrand, Int. J. Mass Spectrom. 197 (2000) 237.
[78] S.G. Lias, J.E. Bartmess, J.F. Libman, J.L. Holmes, R.D. Levin, W.G. Mallard, J. Phys. Chem. Ref. Data 17 (Suppl. 1) (1988).
[79] A.W. Potts, D.M.P. Holland, A.B. Trofimov, J. Schirmer, L. Karlsson, K. Siegbahn, J. Phys. B 36 (2003) 3129.
[80] H.W. Jochims, H. Baumgärtel, S. Leach, Astron. Astrophys. 314 (1996) 1003.
[81] E. Subertova, J. Bok, P. Rihak, V. Prosser, E. Silinsh, Phys. Stat. Sol. (a) 18 (1973) 741.
[82] P.C. Burgers, J.L. Holmes, J.K. Terlouw, J. Am. Chem. Soc. 106 (1984) 2762.
[83] E. Uggerud, H. Schwarz, J. Am. Chem. Soc. 107 (1985) 5046.
[84] M. Inokuti, Rev. Mod. Phys. 43 (1971) 297.
[85] C. Adamo, V. Barone, Chem. Phys. Lett. 274 (1997) 242.
[86] M. Vega-Arroyo, P.R. LeBreton, T. Rajh, P. Zapol, L.A. Curtiss, Chem. Phys. Lett. 380 (2003) 54.
[87] G. Dujardin, S. Leach, O. Dutuit, T. Govers, P.M. Guyon, J. Chem. Phys. 79 (1983) 644.
[88] T. Kobayashi, T. Kubota, K. Ezumi, C. Utsunomiya, Bull. Chem. Soc. Jpn. 55 (1982) 3915.
[89] H.W. Jochims, M. Schwell, J.-L. Chotin, M. Clemino, F. Dulieu, H. Baumgärtel, S. Leach, Chem. Phys. 298 (2004) 279.
[90] S. Denifl, B. Sonnweber, G. Hanel, P. Scheier, T.D. Märk, Int. J. Mass Spectrom. 238 (2004) 47.
[91] B. Coupier, B. Farizon, M. Farizon, M.J. Gaillard, F. Gobert, N.V. de Castro Faria, G. Jalbert, S. Ouaskit, M. Carré, B. Gstir, G. Hanel, S. Denifl, L. Feketeova, P. Scheier, T.D. Märk, Eur. Phys. J. D 20 (2002) 459.
[92] V.I. Zaretskii, V.I. Sadovskaya, N.S. Wulfson, V.F. Sizoy, V.G. Merimson, Org. Mass Spectrom. 5 (1971) 1179.
[93] A. Padva, P.R. LeBreton, R.J. Dinerstein, J.N.A. Ridyard, Biochem. Biophys. Res. Commun. 60 (1974) 1262.
[94] S.D. Wetmore, R.J. Boyd, L.A. Eriksson, Chem. Phys. Lett. 322 (2000) 129.
[95] I.C. Walker, M.H. Palmer, J. Delwiche, S.V. Hoffmann, P. Limao Vieora, N.J. Mason, M.F. Guest, M.-J. Hubin-Franskin, J. Heinesch, A. Giuliani, Chem. Phys. 297 (2004) 289.
[96] H.-E. Audier, M. Fétizon, Y. Henry, T. Prangé, Org. Mass Spectrom. 11 (1976) 1047.
[97] S. Feil, K. Gluch, S. Matt-Leubner, P. Scheier, J. Limtrakul, M. Probst, H. Deutsch, K. Becker, A. Stamatovic, T.D. Märk, J. Phys. B 37 (2004) 3013.
[98] G. Hanel, B. Gstir, S. Denifl, P. Scheier, M. Probst, B. Farizon, E. Illenberger, T.D. Märk, Phys. Rev. Lett. 90 (2003) 188104-1.
[99] Y.-J. Kuan, S.B. Charnley, H.-C. Huang, W.-L. Tseng, Z. Kisiel, Astrophys. J. 593 (2003) 848.
[100] Z. Peeters, O. Botta, S.B. Charnley, R. Ruitenkamp, P. Ehrenfreund, Astrophys. J. Lett. 593 (2003) L129.